

IRRADIATION CREEP BY THE CLIMB-CONTROLLED GLIDE MECHANISM IN PULSED FUSION REACTORS

H. GUROL

*Department of Chemical and Nuclear Engineering, University of California,
Santa Barbara, CA 93106, U.S.A.*

and

N. M. GHONIEM

*School of Engineering and Applied Science, University of California,
Los Angeles, CA 90024, U.S.A.*

(Received February 21, 1980)

The effects of irradiation pulsing on the enhanced climb-glide creep strain are analyzed. A variety of pulsed systems have been studied by analytically modeling the time-dependence of the bulk point-defect concentrations given by the rate theory. Equations for the creep strain are derived for Tokamak-type fusion reactors, pulsed accelerators and inertial confinement fusion reactors, including the effects of mutual point-defect recombination. The creep in pulsed fusion reactors is compared with the creep in systems subject to steady irradiation of equal total dose. It is found that point-defect concentration cycling (due to radiation pulsing) results in enhancement of the irradiation creep strain. In particular, a very large temperature-dependent enhancement is found for inertial confinement fusion reactors. The theoretical results are also compared with experimental data on deuteron irradiated nickel. Good agreement is obtained with the parameters used.

1 INTRODUCTION

The design of fusion reactor structural materials relies strongly on accurate predictions of dimensional changes due to irradiation creep and swelling. In a fusion reactor, the variation of the temperature and displacement rate across the first wall and the blanket can lead to non-uniform dimensional instabilities. Since the first wall restraint mechanism will tend to keep the various parts straight, high stresses can be generated due to non-uniform swelling. Irradiation creep is the mechanism by which stress-relaxation can occur. However, if the amount of irradiation creep is not sufficient for stress-relaxation, or even if non-uniform thermal expansion takes place during the cooling cycle, first wall distortion will lead to a shortened lifetime affecting the fusion reactor plant economics. On the other hand, creep rupture can be a limiting factor to the integrity of the first wall. The importance of irradiation creep prompted a considerable amount of experimental and theoretical research in the last few year.¹⁻¹⁸

One of the major difficulties in understanding the irradiation creep problem is the large number

of proposed mechanisms to explain this phenomenon.¹⁴ While the controversy over the dominant creep mechanism continues in the literature, we will assume in this work that the climb-controlled glide mechanism is responsible for the observable irradiation creep. We base our assumption on the analysis presented by Duffin and Nichols,¹⁵ Nichols,¹⁴ MacEwen and Fidleris¹⁶ and the more recent experimental data of Michel, Hendrick and Pieper,⁸ Simonen and Hendrick,¹⁷ and Vandervoort, *et al.*¹⁸ This does not rule out the possibility of contributions from other mechanisms, especially the stress-induced preferential absorption of point defects (the SIPA mechanism). Extensive investigations of the SIPA mechanism were discussed in the literature by Heald and Speight,¹⁹ Bullough and Willis,²⁰ and Wolfer and Ashkin.²¹

An important point that is worth mentioning here is that the creep rate in both of these mechanisms is controlled by point defect kinetics. The SIPA mechanism depends only on the interstitial flux, whereas the climb-glide model relies on the magnitude of the net point-defect flux impinging on dislocations. Since most of the proposed fusion reactor concepts will probably operate in a

pulsed fashion for a variety of plasma physics and reactor design considerations,²² point defect kinetics will vary from one concept to the other and an irradiation creep response that differs from the steady irradiation equivalent is expected. In a recent experiment by Simonen and Hendrick,¹⁷ it was found that nickel bombarded by a 17 MeV deuteron beam, which was pulsed with a frequency similar to Tokamak designs, exhibits about three times the creep strain of the same material irradiated by a steady source. They also examined the two different creep models discussed above. They concluded that the dominant creep mechanism in their experiment is the climb-glide.²³

The purpose of this paper is to address the question of the effects of radiation pulsing on the enhanced climb-glide creep strain. The modeling of point defect kinetics is accomplished by using approximate analytical treatments, following lines similar to Sizmann²⁴ and Abromeit and Poerschke.²⁵ In Section 2, we consider pulsing under conditions appropriate to Tokamak-type fusion reactors and pulsed accelerators, for the case where point defect recombination is insignificant compared with point defect diffusion to sinks. In Section 3, the effects of recombination are included in the creep equations. The theoretical results are then compared with the experimental data of Simonen and Hendrick.¹⁷ Calculations of the irradiation creep expected in a recent magnetic confinement design (NUWMAK²⁶) are also presented. In Section 4, we formulate the climb-glide creep strain expected for inertial confinement fusion reactors (ICFR's). We again study the effects of including point defect recombination on the creep strain of high damage rate areas, such as near the surface zone of ICFR's.²⁷

Within the rate theory framework, the climb-glide irradiation creep mechanism concerns itself with the behaviour of an *average* dislocation in response to point defect fluxes. This supposition means that every single dislocation will receive an equal net interstitial flux at any point in time. Recently, Mansur, Coghlan and Brailsford²⁸ formulated a cascade diffusion theory where the effects of spatially and temporally discrete production in collision cascades on point defect behavior were investigated. At an observation point such as a dislocation, large fluctuations of point defect temporal concentrations were found to result from the random cascade production in the solid. It seems reasonable then to take the viewpoint that

during one irradiation pulse, especially under ICFR and pulsed accelerator conditions, a cascade is produced close enough to a small group of dislocations enabling them to climb and hence inducing creep strain. A consequence of this argument is that although the *average* climb distance in ICFR's is too small for climb over obstacles due to interstitials during one pulse (Simonen and Hendrick),¹⁷ individual dislocations will still receive large atom fluxes enabling them to climb over obstacles.

Our analysis, particularly in ICFR's, is expected to give an upper bound on the irradiation creep strain by the climb-glide mechanism in pulsed systems. A detailed theoretical investigation with a cascade diffusion theory may be necessary in order to relate the results to intrinsic cascade characteristics. Such a treatment is now under investigation.

The definitions and units of all parameters appearing in the paper are listed in the nomenclature.

2 SINK-DOMINANT CASE

In this section the creep due to cycling of the irradiation will be analyzed under conditions appropriate to Tokamak designs and accelerators, in the case when the mutual point-defect recombination is insignificant. Therefore, the dominant loss mechanism will be the diffusion of the point-defects to sinks in the material. In the sink-dominant case, the temperature is high enough so that diffusion to sinks occurs rapidly, giving rise to low point-defect concentrations and hence minimizing the importance of recombination. However, this need not necessarily involve temperatures high enough for observable swelling, if the sink density is sufficiently high. We shall first derive the creep equation under general conditions and then discuss specific results.

The climb-glide creep rate $\dot{\epsilon}$ is shown by Michel *et al*⁸ to be

$$\dot{\epsilon} = \rho_d \left(\frac{\lambda}{h} \right) b |V_c|.$$

The climb velocity V_c is dependent on the net point-defect flux and is shown by Mansur¹⁰ to be

$$V_c = \frac{2}{3b} (Z_i^A D_i C_i - Z_v^O D_v C_v).$$

Therefore the climb-glide creep rate becomes

$$\dot{\epsilon}(t) = \left(\frac{2}{3} \frac{\lambda}{h} \rho_d \right) |Z_i^A D_i C_i(t) - Z_v^0 D_v C_v(t)|. \quad (1)$$

As note above, the analysis of pulsed creep depends on the knowledge of how the point-defect concentrations vary as a function of time. The rate equations describing bulk point-defect behavior are given by

$$\frac{dC_i(t)}{dt} = P - \alpha C_i C_v - \lambda_i C_i, \quad (2)$$

$$\frac{dC_v(t)}{dt} = P - \alpha C_i C_v - \lambda_v C_v,$$

where λ_i and λ_v are

$$\lambda_i = (Z_i^A \rho_d^A + Z_i^0 \rho_d^N) D_i \quad (3)$$

$$\lambda_v = Z_v^0 D_v \rho_d$$

It is assumed that the dislocations are the only sinks. ρ_d is the total dislocation density, divided between aligned and nonaligned dislocations, ρ_d^A and ρ_d^N , respectively. Recombination can be neglected in Eqs. (2) if (see Sizmann²⁴)

$$4P < \frac{\lambda_i \lambda_v}{\alpha} \quad (4)$$

is satisfied for a given temperature and sink density. The rate Eqs. (2) are then decoupled and can be treated exactly. The cycling of the irradiation will be assumed to have a period T_f , with on-time T_{on} , so that the off-time is $(T_f - T_{on})$.

The response of the vacancies and interstitials to the pulsing will be considerably different. Since the interstitial mean lifetime $\tau_i (= 1/\lambda_i)$ will be very short under all conditions, the interstitials will quickly rise to the steady-state concentration P/λ_i during the on-time. When the irradiation is turned off, $C_i(t)$ will fall very rapidly to its equilibrium concentration. This time-dependence will be exactly duplicated from pulse to pulse (for the interstitials) as shown in Figure 1.

The mean lifetime of the vacancies $\tau_v (= 1/\lambda_v)$ on the other hand can vary from times such that $\tau_v \ll T_f$ to times where $\tau_v > T_f$, depending on the temperature, sink density and the period of the pulsing. For a $\tau_v \ll T_f$, the vacancies rise rapidly to the steady-state value P/λ_v during the on-time, and decay rapidly when the irradiation is turned off. The vacancy concentration profile will be almost identical from one pulse to the next for this case.

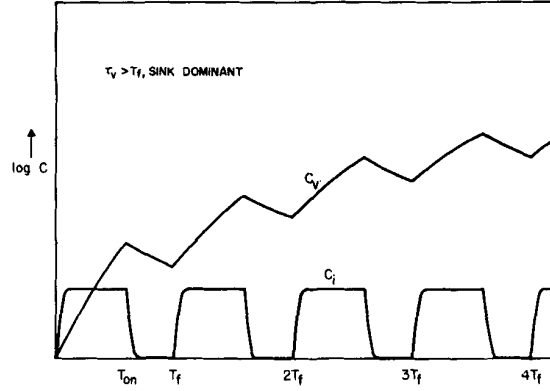


FIGURE 1 Schematic of point-defect concentrations as a function of time for pulsed irradiation, neglecting recombination; $\tau_v > T_f$.

For $\tau_v \approx T_f$, at the end of each pulse there will remain a substantial number of vacancies which have not had sufficient time to diffuse to sinks. When the pulse is turned on again, the vacancy concentration will be enhanced by the diffusing vacancies remaining from previous pulses. This behavior is shown in Figure 1.

The rate Eqs. (2) can now be solved exactly for each pulse by using the appropriate initial conditions (at the beginning of that pulse). The details are shown in Appendix A. During the on-time for the k th pulse, one gets

$$C_v^{(k)}(t) = \frac{P}{\lambda_v} [1 - e^{-\lambda_v(t - [k-1]T_f)}] + \frac{P}{\lambda_v} [1 - e^{-\lambda_v T_{on}}] \sum_{j=0}^{k-2} e^{-\lambda_v(t - [j]T_f + T_{on})} \quad (5a)$$

and

$$C_i^{(k)}(t) = \frac{P}{\lambda_i}, \quad (5b)$$

for $[k-1]T_f < t < [k-1]T_f + T_{on}$.

The superscript k refers to the point-defect concentrations during pulse k . The first term in (5a) is due to the vacancies introduced by the k th pulse. The second term of (5a) gives the vacancy contribution from all the previous pulses. These vacancies are still diffusing to sinks if $\tau_v \approx T_f$. Note that if $\tau_v \ll T_f$, then the second term goes to zero as expected, and there is no

overlapping of pulses. During the off-time of the k th pulse

$$C_v^{(k)}(t) = \frac{P}{\lambda_v} [1 - e^{-\lambda_v T_{\text{on}}}] \sum_{j=0}^{k-1} e^{-\lambda_v(t - [jT_f + T_{\text{on}}])} \quad (6)$$

and

$$C_i^{(k)}(t) \approx 0,$$

for $[k-1]T_f + T_{\text{on}} < t < kT_f$.

Using the expressions (5) and (6) in Eq. (1), the creep rate during the k th pulse becomes

$$\begin{aligned} \dot{\epsilon}_p^{(k)}(t) = & \left(\frac{2\lambda}{3h} P \right) \left\{ \left[\frac{Z_i^A \rho_d}{Z_i^A \rho_d^A + Z_i^0 \rho_d^N} - 1 \right] \right. \\ & \left. + e^{-\lambda_v t} \left[e^{\lambda_v(k-1)T_f} - (e^{\lambda_v T_{\text{on}}} - 1) \sum_{j=0}^{k-2} e^{\lambda_v j T_f} \right] \right\} \end{aligned} \quad (7a)$$

for $[k-1]T_f < t < [k-1]T_f + T_{\text{on}}$, and

$$\dot{\epsilon}_p^{(k)}(t) = \left(\frac{2\lambda}{3h} P \right) \left\{ e^{-\lambda_v t} (e^{\lambda_v T_{\text{on}}} - 1) \sum_{j=0}^{k-1} e^{\lambda_v j T_f} \right\} \quad (7b)$$

for $[k-1]T_f + T_{\text{on}} < t < kT_f$, where we have used the fact that during the on-time $D_i C_i^k(t) > D_v C_v^k(t)$, to eliminate the magnitude in (1). When the pulse is turned off, the interstitial concentration quickly goes to zero, and the resulting creep rate given in Eq. (7b) is due only to the vacancies diffusing to dislocations. The amount of creep contributed by the k th pulse, $\Delta \epsilon_p^{(k)}$, is then given by

$$\begin{aligned} \Delta \epsilon_p^{(k)} = & \int_{[k-1]T_f}^{[k-1]T_f + T_{\text{on}}} \dot{\epsilon}_p^{(k)}(t) dt \\ & + \int_{[k-1]T_f + T_{\text{on}}}^{kT_f} \dot{\epsilon}_p^{(k)}(t) dt. \end{aligned} \quad (8)$$

The total creep after N pulses $\epsilon_p^{(N)}$ can then be evaluated by summing the contributions over all the pulses. That is

$$\epsilon_p^{(N)} = \sum_{k=1}^N \Delta \epsilon_p^{(k)}. \quad (9)$$

Substituting expressions (7a) and (7b) into the respective integrals of (8), and performing the sum indicated by (9) gives the creep as a function

of the number of pulses. The details are presented in Appendix A. The result is

$$\begin{aligned} \epsilon_p^{(N)} = & \left(\frac{2\lambda}{3h} P \right) \left\{ \left[\frac{Z_i^A \rho_d}{Z_i^A \rho_d^A + Z_i^0 \rho_d^N} - 1 \right] N T_{\text{on}} \right. \\ & + N \tau_v (1 - \exp(-\lambda_v T_{\text{on}})) \\ & + N \tau_v (\exp(\lambda_v [T_f - T_{\text{on}}]) - 1) (\exp(\lambda_v T_{\text{on}}) - 1) \\ & \times \exp(-\lambda_v T_f) + [\tau_v (\exp(\lambda_v [T_f - T_{\text{on}}]) - 1) \\ & \times (\exp(\lambda_v T_{\text{on}}) - 1) - \tau_v (1 - \exp(-\lambda_v T_{\text{on}})) \\ & \times \exp(\lambda_v T_f) (\exp(\lambda_v T_{\text{on}}) - 1) \\ & \left. \times \sum_{k=2}^N (N+1-k) \exp(-\lambda_v k T_f) \right\} \end{aligned} \quad (10)$$

This is an analytically exact expression for the creep in a pulsed system as a function of the number of pulses N , in the case when recombination is negligible. In Section (2a) and (2b) we analyze Eq. (10) with respect to TOKAMAK and accelerator designs.

2a Applications to TOKAMAKS

Here we consider the typical TOKAMAK conditions of 230 second burn-time and 15 seconds cooling time, corresponding to the NUWMAK design,²⁶ giving $T_{\text{on}} = 230$ sec., $T_f = 245$ sec. In the previous section, it was seen that the evolution of the pulsed vacancy concentration is governed by the ratio τ_v/T_f . In order to evaluate this ratio the temperature must be specified. For the sink-dominant system under consideration, the temperature must be such that condition (4) is satisfied for a given set of parameters. This condition can be expressed explicitly for the temperature T as

$$T > \frac{E_v^m}{k_B \ln \left[\frac{Z_i^0 (D_i/\alpha) \rho_d^2 D_{v0}}{4P} \right]}. \quad (11)$$

The ratio D_i/α is a constant for a given material. We use the parameters appropriate for stainless steel, shown in Table I. Using these numerical values, condition (11) gives $T > 715$ K. At this temperature (715 K) $\tau_v = 0.26$ seconds, and $\tau_v/T_f \approx 10^{-3}$. As the temperature is increased, τ_v decreases, and the ratio τ_v/T_f is always much less than unity. Therefore, to a very good approximation there will be no overlapping of the vacancy concentration from one pulse to the next, and the time-dependence of vacancies and interstitials will be the same

TABLE I
Material parameters used for stainless steel and nickel

Parameter	Stainless steel	Nickel
Z_i^A	1.125	1.22
Z_i^0	1.025 [29]	1.02 [29]
Z_r^0	1.000	1.000
$D_i^0, m^2/s$	10^{-7} [29]	1.2×10^{-5} [29]
$D_v^0, m^2/s$	5×10^{-5} [29]	6.0×10^{-5} [29]
E_i^m, J	3.2×10^{-20} [29]	2.4×10^{-20} [31]
E_v^m, J	2.1×10^{-19} [29]	1.9×10^{-19} [31]
α		
$\frac{\alpha}{D_i}, m^{-2}$	10^{20} [29]	10^{20} [31]

for every pulse. Physically, this means that the creep contribution of all pulses are the same. This is seen to follow also from Eq. (10) where if the limit $\tau_v/T_f \rightarrow 0$ is taken, one obtains

$$\varepsilon_p^{(N)} \approx \left(\frac{2}{3} \frac{\lambda}{h} P \right) \left\{ \left[\frac{Z_i^A \rho_d}{Z_i^A \rho_d^A + Z_i^0 \rho_d^N} - 1 \right] T_{on} + 2\tau_v \right\} N \quad (12)$$

Notice that the summation term has dropped out and that the creep is simply a linear function of the number of pulses. Assuming that one-third of the dislocations are aligned and two-thirds non-aligned, $\varepsilon_p^{(N)}$ becomes

$$\varepsilon_p^{(N)} \approx \left(\frac{2}{3} \frac{\lambda}{h} P \right) \left\{ 2 \left(\frac{Z_i^A - Z_i^0}{Z_i^A + 2Z_i^0} \right) T_{on} + 2\tau_v \right\} N \quad (13)$$

However, since $\tau_v \ll T_{on}$ for the sink-dominant case, the τ_v term does not play a significant role. The first term in Eq. (13) is of course just the steady irradiation creep during the time T_{on} as outlined in Appendix B. Since τ_v is small, the vacancy concentration rapidly decays during the off-time, giving almost no contribution to the creep. Hence for a sink-dominant Tokamak, the pulsed creep will be virtually identical to the steady-irradiation creep. To show the insensitivity of the creep to varying τ_v/T_f , we have shown in

Table II $\varepsilon_p^{(N)}$ for values of τ_v/T_f ranging from 10^{-3} to 10^{-5} , for 100 pulses.

2b Application to Pulsed Accelerators

Ion beam accelerators are used in radiation damage experiments due to the high degree of flexibility in controlling the material irradiation parameters. Damage rates ranging from 6×10^{-7} dpa/s¹⁷ up to 0.32 dpa/s³⁴ have been experimentally achieved. On the other hand, pulsed accelerator experiments were conducted for on-times in the range of 2.5×10^{-5} seconds³⁴ up to 1000 seconds.¹⁷ In order to illustrate the sensitivity of the creep strain to the pulsing conditions, we have chosen to analyze a proposed experiment with the following parameters: $T_{on} = 0.023$ seconds, $T_f = 0.0245$ seconds, $P = 10^{-6}$ dpa/s and $\rho_d = 10^{14} m^{-2}$. These parameters are chosen in order to represent an experimental simulation of the NUWMAK design, with the cycle times scaled down by a factor of 10^4 . During the much shorter cycling times in the proposed experiment, the vacancy concentration will not follow the time behavior of point defect production. The effects of defect accumulation from one pulse to the next can therefore be investigated. It should be also noted that the creep component analyzed in this work is only due to the irradiation induced climb-glide dislocation motion, and that the creep strain arising from vacancy emission from the network has to be added in the high temperature range.²⁰ This thermal component is expected to be independent of the time behaviour of irradiation produced defects.

Figure 2 shows the creep strain corresponding to the pulsed accelerator conditions as a function of the number of pulses. At 715 K, τ_v is about 10 times T_f , giving rise to a strain transient due to an overlap of the vacancy concentrations in successive pulses. This transient extends for ~ 20 – 30 pulses. The strain rate during this transient is large, since the interstitial flux ($D_i C_i$) is much higher than the vacancy flux until ~ 2 – $3 \tau_v$. On the

TABLE II
Irradiation creep results for the sink-dominant TOKAMAK case ($\rho_d = 10^{14}/m^2$, $P = 10^{-6}$ dpa/sec)

Temp. K	τ_v , sec.	τ_v/T_f	$\Delta\varepsilon_p$ (creep/pulse)	ε_p^{100} , m/m	ε_{ss} , at $N = 100$, m/m
715	0.24	$\sim 10^{-3}$	1.057×10^{-4}	1.057×10^{-2}	1.023×10^{-2}
804	0.023	$\sim 10^{-4}$	1.027×10^{-4}	1.027×10^{-2}	1.023×10^{-2}
916	0.0023	$\sim 10^{-5}$	1.024×10^{-4}	1.024×10^{-2}	1.023×10^{-2}

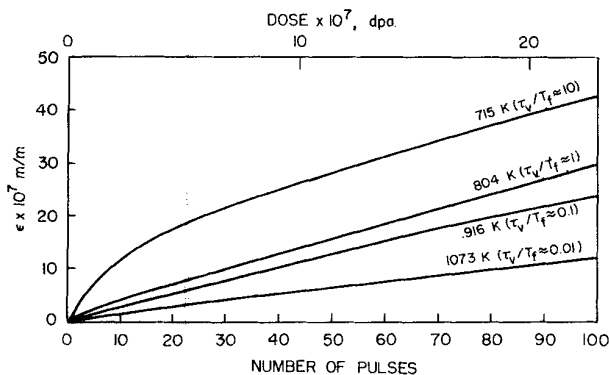


FIGURE 2 The creep as a function of the number of pulses for pulsed accelerator conditions, neglecting recombination, for different temperatures.

other hand, the vacancy concentration does not decay appreciably during the off-time, and therefore adds an extra contribution to the total creep strain. As the irradiation temperature gets higher, the transient part of the curve becomes less pronounced and the creep rate during the linear part decreases (slope of the straight line). The results are summarized in Figure 3, where the average creep rate during a certain number of pulses, N , is given as a function of irradiation temperature. The average creep strain is obtained by dividing the total strain after N pulses by the total dose

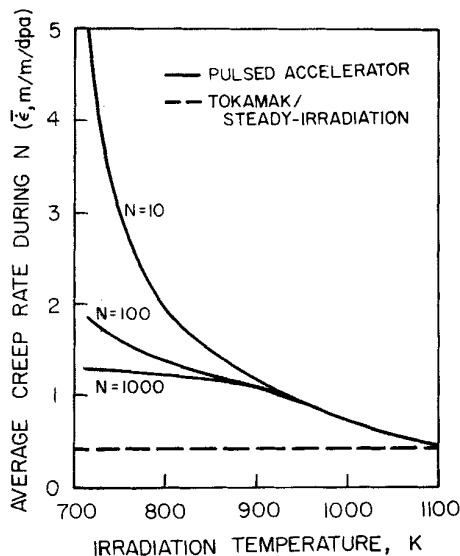


FIGURE 3 The average creep rate as a function of irradiation temperature, for different numbers of pulses.

accumulated during the same number of pulses. At the low temperature end, the average creep rate is high and decreases to a saturation value at large N . The average strain rate decreases with increasing temperature reaching the constant value of $\sim 0.46 \text{ dpa}^{-1}$ achieved during the TOKAMAK or steady-irradiation conditions as discussed in the previous section. Although we do not intend to compare the results of this section to experimental data, it is interesting to note that during the recent transient creep experiment of Michel *et al.* on nickel,⁸ creep strain rates of 4.5 dpa^{-1} down to 0.06 dpa^{-1} were observed at 497 K.

3 GENERAL CASE OF POINT-DEFECT KINETICS INCLUDING DIFFUSION AND MUTUAL RECOMBINATION

In the present context, condition (11) is not satisfied. The temperature is low enough then, that the point-defect kinetics is no longer dictated by the sinks alone, but by a combination of diffusion to sinks and mutual recombination. Mathematically, this means that the rate Eqs. (2) are no longer decoupled. In order to proceed analytically we will model the time-dependence of the point defects under cyclic irradiation. Sizmann²⁴ and Abromeit and Poerschke²⁵ have obtained approximate solutions to the rate equations by defining distinct time regimes in the build-up of the vacancy and interstitial concentrations from their initial thermal

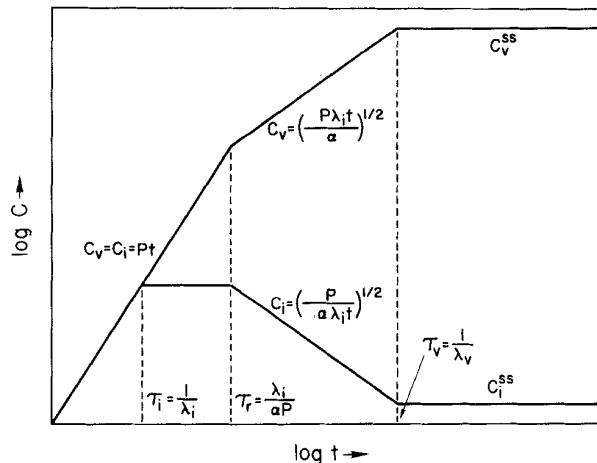


FIGURE 4 Approximate variation of the point-defect concentrations as a function of time for the low temperature, high sink density case (courtesy of R. Sizmann²⁴).

equilibrium values (the irradiation is turned on at $t = 0$) to their steady-state values. Sizmann does this for a variety of "high" and "low" temperatures and sink concentrations.

Figure 4 shows the approximate variations of $C_v(t)$ and $C_i(t)$ in the various times regimes for the low temperature, high sink case, of interest in this section. In reality of course, the transition from one regime to the next is smooth, without the abrupt changes at the transition points, as treated by Abromeit and Poerschke.²⁵ Initially, when the irradiation is first turned on, there are no losses and $C_v(t)$, $C_i(t)$ increase linearly in time. After a time τ_i , the interstitials start diffusing to sinks and reach an intermediate steady-state concentration. However, the vacancies are still building up linearly since on the average they have not been able to diffuse to sinks yet, and there are not enough of them for appreciable recombination. When $C_v(t)$ has reached a high enough value (at time τ_r), mutual recombination starts playing an important role. It can be shown quite readily by neglecting vacancy diffusion to sinks in the rate Eqs. (2), that approximately $C_v(t) \propto t^{1/2}$ and $C_i(t) \propto t^{-1/2}$. Once a significant number of vacancies have started to diffuse to sinks at time τ_v , both C_v and C_i reach their steady-state values. Hence, it is the vacancy diffusion to sinks which determines when steady-state concentrations will ultimately be reached.

Under cyclic irradiation, the above depicted behavior will be interrupted. The resulting variation of the point-defect concentrations will depend on how the time of approach to steady-state, that is τ_v , compares with the total observation time, NT_f . τ_v depends, of course, on the temperature and the sink density, but its value is also extremely sensitive to the vacancy migration energy used. There are two cases of interest: $\tau_v > NT_f$ and $\tau_v < T_{on}$. Let us first examine $\tau_v > NT_f$.

3a $\tau_v > NT_f$: Transient Vacancy Behavior for all Pulses

The effect of interrupting the irradiation on the vacancy and interstitial concentration is shown in Figure 5, for the situation of a large τ_v . By referring to Figures 4 and 5, we see that during the first pulse $C_v(t)$ rises linearly until time τ_r , whereafter it assumes a $t^{1/2}$ dependence until the pulse is turned off at $t = T_{on}$. During the off-time it remains virtually unchanged since τ_v is large. When the irradiation is turned on again at the

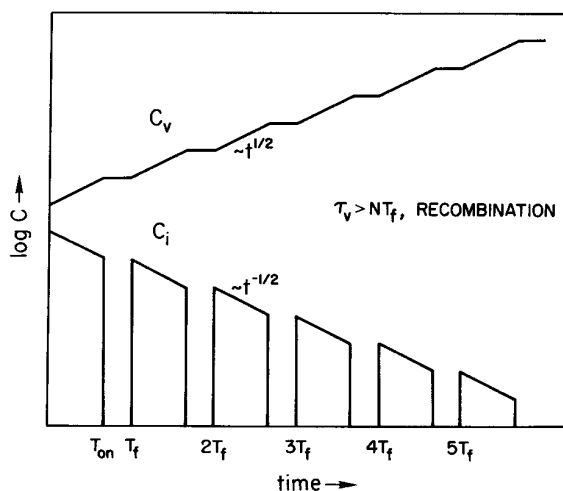


FIGURE 5 Schematic of point-defect concentrations as a function of time for pulsed irradiation, including recombination; $\tau_v > NT_f$.

beginning of the second pulse, $C_v(t)$ picks up from almost exactly where it left off at $t = T_{on}$ and is proportional to $t^{1/2}$. Now since τ_v is taken to be longer than the total observation time NT_f , the vacancy concentration will never reach its steady-state value. Therefore for pulses 2 through N , the vacancies grow as $t^{1/2}$ during the on-times and are constant to a good approximation during the off-times. The vacancy concentration for the k th pulse can be shown to be given by

$$C_v^{(k)}(t) = \left(\frac{P\lambda_i}{\alpha} \right)^{1/2} (t - (k-1)[T_f - T_{on}])^{1/2},$$

$$[k-1]T_f < t < [k-1]T_f + T_{on} \quad (14)$$

and

$$C_v^{(k)}(t) = \left(\frac{P\lambda_i T_{on}}{\alpha} \right)^{1/2} k^{1/2},$$

$$[k-1]T_f + T_{on} < t < kT_f, k \geq 2.$$

During the first pulse, the interstitials rise very rapidly to the intermediate steady-state concentration, which they keep until $t = \tau_r$. Past τ_r , the interstitial concentration declines as $t^{-1/2}$, and when the first pulse is turned off, $C_i(t)$ rapidly goes to its very low thermal equilibrium value. The point defect concentrations are almost entirely dictated by mutual recombination and therefore the concentration of one can be determined by knowing the other. Since $C_i(t)$ did not change

appreciably during the off-time, then $C_i(t)$ must resume the value it had at the end of the preceding pulse, and continue to decline as $t^{-1/2}$. This behavior will be repeated by the interstitials for all pulses past the second, the interstitials never reaching their steady-state value, since the time to steady state τ_v is dictated by the vacancies diffusing to sinks. For the k th pulse, where $k \geq 2$, the interstitial concentration is given by

$$C_i^{(k)}(t) = \left(\frac{P}{\alpha\lambda_i}\right)^{1/2} (t - (k-1)[T_f - T_{\text{on}}])^{-1/2},$$

$$[k-1]T_f < t < [k-1]T_f + T_{\text{on}} \quad (15)$$

and $C_i^{(k)}(t) = 0$, $[k-1]T_f + T_{\text{on}} < t < kT_f$.

Using (14) and (15) in Eq. (1), the creep rate during pulse k becomes

$$\dot{\epsilon}_p^{(k)}(t) = \left(\frac{2\lambda}{3h}\rho_d\right) \times \left\{ Z_i^A D_i (t - (k-1)[T_f - T_{\text{on}}])^{-1/2} \left(\frac{P}{\alpha\lambda_i}\right)^{1/2} - Z_v^0 D_v \left(\frac{P\lambda_i}{\alpha}\right)^{1/2} (t - (k-1)[T_f - T_{\text{on}}])^{1/2} \right\}$$

$$(16a)$$

for $[k-1]T_f < t < [k-1]T_f + T_{\text{on}}$, and

$$\dot{\epsilon}_p^{(k)}(t) = \left(\frac{2\lambda}{3h}\rho_d\right) Z_v^0 D_v \left(\frac{P\lambda_i}{\alpha}\right)^{1/2} T_{\text{on}}^{1/2} k^{1/2} \quad (16b)$$

for $[k-1]T_f + T_{\text{on}} < t < kT_f$.

In order to eliminate the magnitude appearing in Eq. (1), we have again used the fact that the interstitial flux $D_i C_i^{(k)}(t)$ is always greater than the vacancy flux $D_v C_v^{(k)}(t)$ during the on-times. The contribution to the creep during the off-times comes only from the vacancies as expressed by Eq. (16b). Using Eq. (8), the amount of creep contributed by pulse k , $\Delta\epsilon_p^{(k)}$, can now be evaluated. Then the total creep after N pulses is given by

$$\epsilon_p^{(N)} = \Delta\epsilon_p^{(1)} + \sum_{k=2}^N \Delta\epsilon_p^{(k)}. \quad (17)$$

Leaving the details of the manipulations to Appendix C, we find

$$\epsilon_p^{(N)} \approx \left(\frac{4\lambda}{3h}\rho_d\right) \left\{ Z_i^A D_i \left(\frac{PT_{\text{on}}}{\alpha\lambda_i}\right)^{1/2} (N^{1/2} - 1) - \frac{1}{3} Z_v^0 D_v \left(\frac{P\lambda_i T_{\text{on}}}{\alpha}\right)^{1/2} [2T_{\text{on}} - T_f] (N^{3/2} - 1) \right\} + \Delta\epsilon_p^{(1)} \quad (18a)$$

and

$$\Delta\epsilon_p^{(1)} = \left(\frac{2\lambda}{3h}\rho_d\right) \left\{ Z_i^A D_i \times \left[\frac{P}{\lambda_i} \tau_r + 2 \left(\frac{P}{\alpha\lambda_i}\right)^{1/2} (T_{\text{on}}^{1/2} - \tau_r^{1/2}) \right] - Z_v^0 D_v \times \left[\frac{P\tau_r^2}{2} + \left(\frac{P\lambda_i}{\alpha}\right)^{1/2} \left(\frac{5}{3} T_{\text{on}}^{3/2} - \frac{2}{3} \tau_r^{3/2} - T_{\text{on}}^{1/2} T_f \right) \right] \right\} \quad (18b)$$

In order to shed more light on the physical implications of Eqs. (18a) and (18b), we note from Eqs. (16a) and (16b) that $\epsilon_p^{(N)}$ can be written as the sum of the creep contributions during the on-time and off-time. That is

$$\epsilon_p^{(N)} = \epsilon_{\text{on}}^{(N)} + \epsilon_{\text{off}}^{(N)},$$

where

$$\epsilon_{\text{on}}^{(N)} = \left(\frac{4\lambda}{3h}\rho_d\right) \left\{ Z_i^A D_i \left(\frac{PT_{\text{on}}}{\alpha\lambda_i}\right)^{1/2} (N^{1/2} - 1) - \frac{1}{3} Z_v^0 D_v \left(\frac{P\lambda_i T_{\text{on}}}{\alpha}\right)^{1/2} T_{\text{on}} (N^{3/2} - 1) \right\} \quad (19)$$

and

$$\epsilon_{\text{off}}^{(N)} = \left(\frac{2\lambda}{3h}\rho_d\right) Z_v^0 D_v \left(\frac{P\lambda_i T_{\text{on}}}{\alpha}\right)^{1/2} (T_f - T_{\text{on}}) \sum_{k=2}^N k^{1/2} \quad (20)$$

Expression (20) for $\epsilon_{\text{off}}^{(N)}$ has been written in its more exact form using the summation. Whereas in Eq. (18) above we have replaced the sum by an integral which can be evaluated. This, however, is an excellent approximation and can be used for virtually all values of N (see Appendix C).

To investigate the pulsed creep of the present case, stainless steel with a dislocation density of 10^{14} m^{-2} , $T_{\text{on}} = 1000 \text{ sec.}$, and $T_f = 1100 \text{ sec.}$ was considered for two different temperatures. The complete list of parameters is given in Table I. The pulsed creep as a function of the number of pulses has been plotted using Eq. (18) for the two temperatures with corresponding values of τ_v , ranging from 10^5 to 10^6 sec. To compare steady irradiation versus pulsed creep, Figure 6 also shows the steady creep for $T = 390^\circ\text{K}$ and $T = 415^\circ\text{K}$. The steady irradiation creep has been evaluated by using Eq. (1) in conjunction with point-defect equations given by Sizmann²⁴ and indicated in Figure 4. Of course, to make the comparisons meaningful, we have chosen the

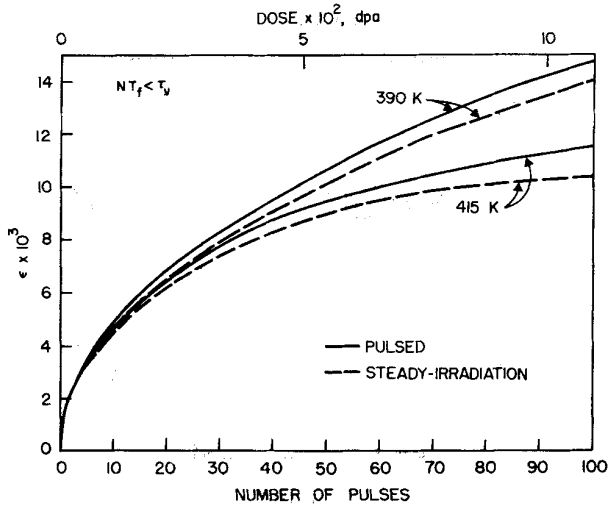


FIGURE 6 The creep strain as a function of time for pulsed and steady irradiation, including recombination; $\tau_v > NT_f$.

damage rates so that the total damage accumulated at any time is identical for the steady and pulsed cases. First, it is seen that increasing the temperature gives rise to less creep. This can be understood by looking at the temperature dependent quantities in Eqs. (19) and (20). The quantity (α/D_i) is a constant which we define as L . Then $\epsilon_{\text{off}}^{(N)}$ and $\epsilon_{\text{on}}^{(N)}$ can be rewritten as

$$\epsilon_{\text{on}}^{(N)} = \left(\frac{4\lambda}{3h} \rho_d \right) \left\{ Z_i^A \left(\frac{PT_{\text{on}}}{Z_i^0 L \rho_d} \right)^{1/2} (N^{1/2} - 1) - \frac{1}{3} Z_v^0 D_v(T) \left(\frac{PT_{\text{on}} Z_i^0 \rho_d}{L} \right)^{1/2} T_{\text{on}} (N^{3/2} - 1) \right\} \quad (21)$$

$$\epsilon_{\text{off}}^{(N)} = \left(\frac{2\lambda}{3h} \rho_d \right) Z_v^0 D_v(T) \left(\frac{PT_{\text{on}} Z_i^0 \rho_d}{L} \right)^{1/2} \times (T_f - T_{\text{on}}) \sum_{k=2}^N k^{1/2} \quad (22)$$

It is noted that within the framework of the current calculations, the only explicit temperature dependence is that of the vacancy diffusion coefficient. Increasing the temperature increases $D_v(T)$, which has the effect of decreasing $\epsilon_{\text{on}}^{(N)}$ and increasing $\epsilon_{\text{off}}^{(N)}$ as seen from Eqs. (21) and (22). However, because the off-time $(T_f - T_{\text{on}})$ is only a fraction of T_{on} in this example, the net effect on the creep $\epsilon_p^{(N)}$ is a decrease with temperature. The same comments apply to steady irradiation creep. In this case, the creep is then given by Eq. (21) alone, with a redefined damage rate to conserve the total damage. Again it is seen that increasing

the temperature gives rise to decreased creep. A comparison of steady versus pulsed creep shows that pulsed creep is always somewhat greater than steady irradiation, the difference between the two being greater with increasing temperature. The reasons for these results can be explained as follows. Under steady irradiation, the creep rate is simply given as the difference between the interstitial and vacancy fluxes. However, when the irradiation is pulsed, during the off-time the vacancies contribute an amount $\epsilon_{\text{off}}^{(N)}$ given by (22). It is this *additive* contribution during the pulse off-time which gives rise to the enhanced creep under pulsing. Furthermore, increasing the temperature will increase "off-time creep" $\epsilon_{\text{off}}^{(N)}$, giving rise to a greater difference between the steady and pulsed cases.

In Figure 7 we investigate the effects of varying the ratio τ_v/NT_f on the creep $\epsilon_p^{(N)}$, for $T = 415$ K. It is seen that for $\tau_v \approx 4NT_f$, the creep after N pulses becomes independent of τ_v . That is, once the temperature is low enough so that $\tau_v \approx 4NT_f$, the creep is the same for all lower temperatures (and higher τ_v). This is also evident from Eqs. (21) and (22), where it can be seen that for large τ_v and a fixed dislocation density, the diffusion rate of the vacancies to dislocations within one pulse is very low and hence one can neglect the vacancy contribution during the on- and off-time, and Eq. (18) simplifies to

$$\epsilon_p^{(N)} \approx \epsilon_{\text{on}}^{(N)} \approx \left(\frac{4\lambda}{3h} \rho_d \right)^{1/2} \left(\frac{PT_{\text{on}}}{Z_i^0 L} \right)^{1/2} \times (N^{1/2} - 1) Z_i^A, \quad (23)$$

which is valid for $\tau_v \approx 4NT_f$.

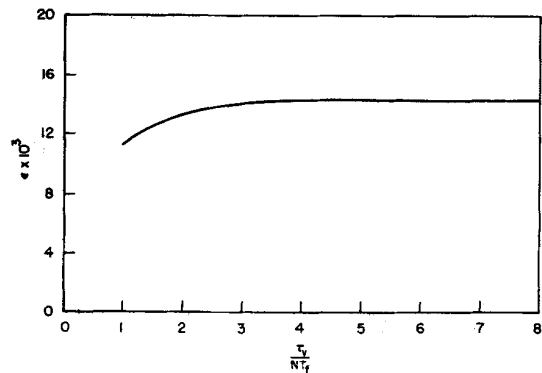


FIGURE 7 Variation of the pulsed creep strain as a function of the ratio τ_v/NT_f , including recombination for $T = 415$ K.

To investigate the effect of changing the percentage off-time, we have considered equal on- and off-times of 100 sec., with a damage rate of $P = 2 \times 10^{-6}$ dpa/sec., chosen so as to give equal accumulated damage with the example of Figure 6. For equal on- and off-times, $T_f = 2T_{on}$, and we see from Eq. (18) that the vacancy contribution goes to zero giving just

$$\epsilon_p^{(N)} = \left(\frac{4}{3} \frac{\lambda}{h} \rho_d \right) Z_i^A D_i \left(\frac{PT_{on}}{\alpha \lambda_i} \right)^{1/2} (N^{1/2} - 1). \quad (24)$$

Using $L = (\alpha/D_i) = \text{constant}$, one gets the temperature-independent result, Eq. (23). This means that the pulsed creep resulting from the case $\tau_v \lesssim 4NT_f$ is the same as the creep that occurs when one has equal on- and off-times. In both cases the effect of the vacancies goes to zero and the creep is due to the interstitials alone. Figure 8 shows the contribution of the vacancies and interstitials to the creep rate during the on- and off-times (for $2T_{on} = T_f$) by using Eqs. (1), (16a) and (16b). It is seen that there is a small initial difference in the effect of the vacancies during the on- and off-times, but that after about 50 pulses, the two become identical, the creep due exclusively to the interstitials. The resulting creep $\epsilon_p^{(N)}$ is also plotted. By comparison with Figure 6 ($T = 415^\circ\text{K}$), it is observed that cyclic irradiation with the greater percentage off-time (and all other parameters equal) results in greater creep for equal total amounts of damage. For example, 400 pulses in Figure 8 corresponds to about 72 pulses in Figure 6 with respective values of creep of about 13×10^{-3} and 11×10^{-3} . This small difference of 2×10^{-3} can once again be attributed to the additive contribution of the vacancies to the creep during the off-time. For equal on- and off-times, the vacancy terms cancel each other when Eqs. (21) and (22) are added. If the off-time is less than the on-time, the contribution of the vacancies (during the off-time) Eq. (22), is still added to Eq. (21). But its effect is now smaller and cannot cancel the vacancy term in $\epsilon_{on}^{(N)}$.

3b $\tau_v < T_{on}$: Steady-State Achieved During the On-Time

The characteristic feature of small values of τ_v is that the vacancies and interstitials are able to reach their steady-state concentrations during a single pulse. The effect of interrupting the irradiation (for $\tau_v < T_{on}$) is shown in Figure 9, which

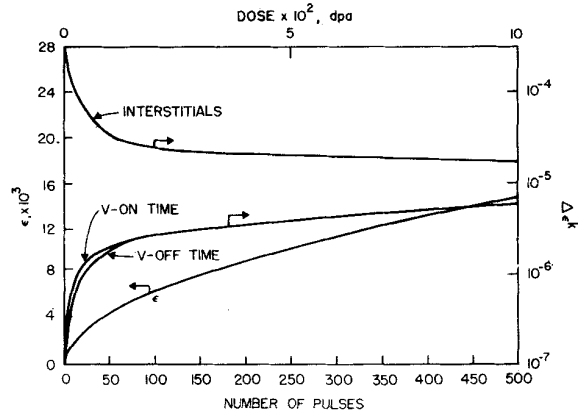


FIGURE 8 Contribution to the creep strain of the vacancies and interstitials during the irradiation and annealing times as a function of the number of pulses.

once again has been drawn by using the approximate solutions to the rate equations,²⁴ depicted in Figure 4. During the first pulse, $C_v(t)$ rises linearly until time τ_r , after which it becomes proportional to $t^{1/2}$. At time τ_v , it reaches its steady-state concentration C_v^{ss} , and remains at this value until the pulse is turned off. During the off-time, the vacancies decay exponentially. When the second pulse is turned on, the time-dependence of $C_v(t)$ will depend on how much the vacancy concentration has decayed during the off-time. If τ_v is very small, $C_v(T_f)$ may be so low as to correspond to a concentration below $t = \tau_r$ in the first pulse, giving a linear time dependence. However, the values of τ_v characteristic of TOKAMAK designs and pulsed experiments are usually longer than τ_r . Therefore the concentration at the beginning of

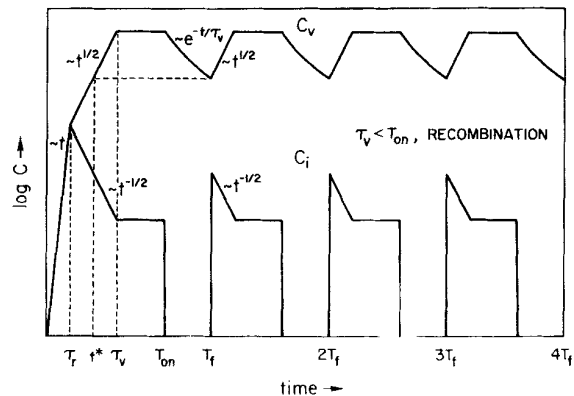


FIGURE 9 Schematic of point-defect concentrations as a function of time for pulsed irradiation, including recombination: $\tau_v < T_{on}$.

pulse 2, $C_v^{(2)}(T_f)$, will be equal to a concentration that corresponds to a time t^* in the first pulse. Then $C_v^{(2)}(t)$ grows as $t^{1/2}$ for a length of time $\tau'_v \equiv \tau_v - t^*$, after which it reaches steady-state, and then decays exponentially when the pulse is off. Of course it decays to the same value of $C_v(t)$ as at the end of the first pulse. Therefore, after the first pulse, all the others are identical. The vacancy concentration for the k th pulse is then given by

$$C_v^{(k)}(t) = \left(\frac{P\lambda_i}{\alpha}\right)^{1/2} (t - (k-1)[T_f - t^*])^{1/2},$$

$$[k-1]T_f < t < [k-1]T_f + \tau'_v$$

$$C_v^{(k)}(t) = C_v^{ss},$$

$$[k-1]T_f + \tau'_v < t < [k-1]T_f + T_{on} \quad (25)$$

and

$$C_v^{(k)}(t) = C_v^{ss} \exp[-\lambda_v(t - [k-1]T_f - T_{on})],$$

$$[k-1]T_f + T_{on} < t < kT_f$$

valid for $k \geq 2$.

The same logic can now be applied to the interstitials. Past $t = \tau_r$, the interstitials have a $t^{-1/2}$ dependence, which they maintain until τ_v when they reach the steady state concentration C_i^{ss} . When the irradiation is turned off, the interstitials decay almost instantly to their thermal equilibrium value. When the second pulse is turned on, they then quickly rise to the concentration C_i which corresponds to the vacancy concentration at time T_f . Since $C_v^{(2)}(T_f)$ is $\propto t^{1/2}$, $C_i^{(2)}(T_f)$ will go as $t^{-1/2}$. Starting with the second pulse, the interstitials will follow the same profile from pulse to pulse. Therefore, the interstitial concentration for pulse k is given by

$$C_i^{(k)}(t) = \left(\frac{P}{\alpha\lambda_i}\right)^{1/2} (t - (k-1)[T_f - t^*])^{-1/2},$$

$$[k-1]T_f < t < [k-1]T_f + \tau'_v$$

$$C_i^{(k)}(t) = C_i^{ss},$$

$$[k-1]T_f + \tau'_v < t < [k-1]T_f + T_{on} \quad (26)$$

$$C_i^{(k)}(t) = 0, [k-1]T_f + T_{on} < t < kT_f$$

valid for $k \geq 2$.

The time t^* can be simply calculated by equating the concentration at the beginning of pulse 2 with that concentration in pulse 1, obtained by the intersection of the horizontal line shown in Figure 9. The result is (see Appendix D for details)

$$t^* = f \tau_v, \quad (27)$$

where $f \equiv \exp[-2\lambda_v(T_f - T_{on})] < 1$.

Since the point-defect histories are repeated from pulse to pulse, only a single pulse needs to be considered to evaluate the creep. Following the basic approach of previous sections, the creep rate in the three regions of each pulse can be evaluated. After straightforward integration, the creep at the end of N pulses becomes

$$\epsilon_p^{(N)} = N\Delta\epsilon_p = N\left(\frac{2\lambda}{3h}\rho_d\right)\left\{2Z_i^A D_i \left(\frac{P}{\alpha\lambda_i}\right)^{1/2}\right.$$

$$\times (\tau_v^{1/2} - t^{*1/2}) - \frac{2}{3} Z_v^0 D_v \left(\frac{P\lambda_i}{\alpha}\right)^{1/2} (\tau_v^{3/2} - t^{*3/2})$$

$$+ [Z_i^A D_i C_i^{ss} - Z_v^0 D_v C_v^{ss}](T_{on} - \tau'_v)$$

$$\left. + \frac{C_v^{ss}}{\rho_d} (1 - \exp[-\lambda_v(T_f - T_{on})])\right\}. \quad (28)$$

The creep is linear in N , since the creep per pulse, $\Delta\epsilon_p$ is the same for all pulses.

Recently, Simonen and Hendrick¹⁷ have measured the irradiation creep of deuteron irradiated nickel subject to 1000 sec. on-time, followed by 100 sec. of annealing. They concluded that the dominant (radiation induced) creep mechanism is climb-glide and not SIPA. Furthermore, their measurements show that the pulsed creep rate is approximately three times the creep rate with steady irradiation. In order to see if the above pulsed climb-glide model is able to approximately reproduce the experimental observations, we have used parameters appropriate for nickel and those given by Simonen and Hendrick¹⁷ in Eq. (28). The complete list of parameters used is listed in Table I. Following the analysis of Ref. 17 we have assumed a total dislocation density of $3 \times 10^{14}/\text{m}^2$, with one-third having an aligned orientation relative to the stress axis. For $T = 477^\circ\text{K}$, one finds that $\tau_v \approx 252$ sec., so that the present analysis ($\tau_v < T_{on}$) is indeed the proper one. For the list of nickel parameters used, it is seen in Figure 10 that one does observe a three-fold enhancement of the creep in the pulsed case; furthermore, the magnitude of the creep agrees well with the measurement of Simonen and Hendrick.¹⁷ The parameter values we have used are reasonable for nickel, however it should be realized that these parameters are not exactly known, and their numerical values actually fall in a range. Since the time of vacancy diffusion to sinks τ_v , dictates much of the physics, the vacancy pre-exponential D_v^0 and especially the vacancy migration energy E_v^m affect the results significantly. Since E_v^m appears

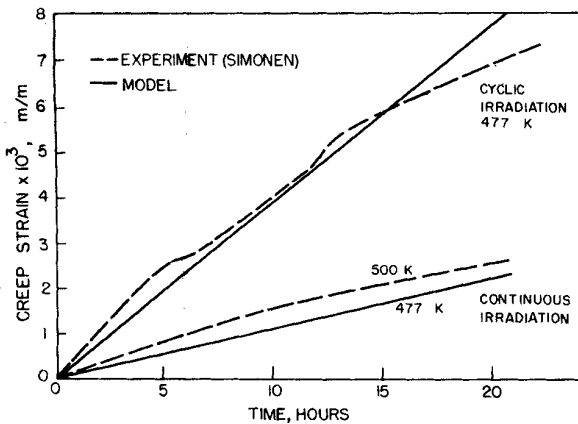


FIGURE 10 Comparison of the creep strain using the analytical model (Eq. 28) with experimental measurement,¹⁷ as a function of time.

in an exponential, a small difference in the value of E_v^m can bring about order-of-magnitude changes in the value of τ_v , possibly implying completely different pulsed point-defect behavior. Therefore, the only claim that can safely be made is that Eq. (28) with the parameters used (which appear reasonable) satisfactorily describes the creep and the enhancement observed by Simonen and Hendrick.¹⁷

We have also investigated the pulsed creep of 316 stainless steel subject to pulsing appropriate to the NUWMAK design²⁶ using Eq. (28). A total on-time of 230 sec., with a 15 sec. annealing time was used. The other parameters are listed in Table I. Two temperatures were chosen to give the corresponding values of τ_v equal to $0.2T_{on}$

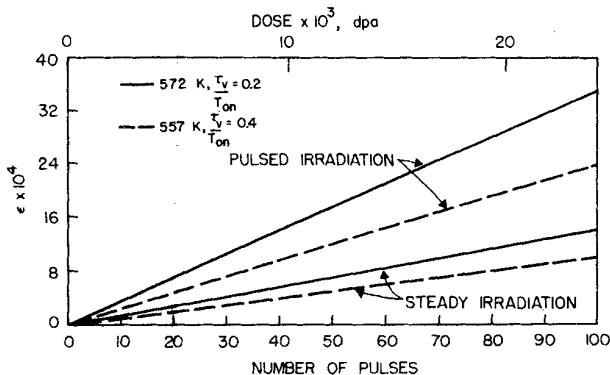


FIGURE 11 The creep strain as a function of time for pulsed and steady irradiation, with NUWMAK parameters.

and $0.4T_{on}$, respectively. It can be seen that a substantial enhancement of the creep can be expected in this design as compared with the steady irradiation case (Figure 11).

The enhancement in these calculations can be explained by looking at the contributions to the creep in Eq. (28). From Eq. (28), the creep during a single pulse can be written as the sum of three parts:

$$\Delta\epsilon_p = \Delta\epsilon_p^A + \Delta\epsilon_p^{ss} + \Delta\epsilon_p^{off}$$

$\Delta\epsilon_p^A$ is the creep during the approach to the steady-state point-defect concentrations; here the vacancies and interstitials exhibit $t^{1/2}$ and $t^{-1/2}$ behavior, respectively. $\Delta\epsilon_p^{off}$ is the creep resulting from the pulse off-time. $\Delta\epsilon_p^A$ and $\Delta\epsilon_p^{ss}$ contain the difference between the interstitial and vacancy fluxes. $\Delta\epsilon_p^A$ is greater than the corresponding steady irradiation creep due to the transient interstitial behavior. $\Delta\epsilon_p^{off}$ contains only the vacancy flux, since upon turning the irradiation off, the interstitials almost instantly reach their thermal equilibrium concentration. It is this additive contribution of the vacancies in $\Delta\epsilon_p^{off}$ and the enhancement of $\Delta\epsilon_p^A$ due to the interstitials which are responsible for the enhancement of the creep in these pulsed systems.

4 IRRADIATION CREEP IN ICFR'S

In Inertial Confinement Fusion Reactors (ICFR's), the displacement damage in the first wall material occurs during a very short time defined as the on-time (T_{on}), after which the solid is allowed to relax until the next damage pulse arrives after the period T_f . In order to investigate the creep rate and total creep strain in the first wall material after the accumulation of a large number of pulses, we will develop approximate analytical expressions for point defect concentrations. Point defect behavior will be first analyzed for the case when mutual recombination is insignificant, and then will be followed by including mutual point defect recombination.

During the damage pulse, T_{on} , point defect concentrations increase linearly as a function of time. The very short pulse interval (10^{-9} – 10^{-6} sec.²⁷) does not allow significant diffusion to existing sinks, or even mutual recombination. T_{on} is typically shorter than the interstitial mean lifetime, τ_i , and the mutual recombination time

constant, τ_r , as defined by Sizmann.²⁴ The fractional concentrations can then be described by:

$$C_v = C_i = \left(\frac{PT_f}{T_{on}}\right)t, 0 \leq t \leq T_{on} \quad (29)$$

At the end of the damage pulse, point defect concentrations reach the values:

$$C_v = C_i = PT_f \quad (30)$$

Once the source of irradiation is turned off, point defects start their interactions through mutual recombination and diffusion to various sinks. The describing kinetic equations are then given by Eqs. (2) of Section 2, with $P = 0$.

4a Sink-Dominant Case

The two non-linear Eqs. (2) can be greatly simplified if the interstitial sink removal rate at the end of the damage is greater than the recombination rate at the same instant. This is satisfied if

$$\frac{1}{\alpha\tau_i} > PT_f \quad (31)$$

Point defect concentrations at any time (t) from the start of the off-time of the k th pulse are then given by Ref. 30:

$$C_i^{(k)}(t) = PT_f e^{-t/\tau_i} \quad (32)$$

$$C_v^{(k)}(t) = PT_f(1 + S_k)e^{-t/\tau_v} \quad (33)$$

where

$$S_k = \sum_{j=1}^{k-1} (\tilde{\eta}_v)^j, \quad (34)$$

and

$$\tilde{\eta}_v = e^{-T\tau/\tau_v},$$

and

$$t' \equiv t - T_{on}. \quad (35)$$

As has been discussed in the introduction, an upper bound on the creep rate is expected to result from the rate formulation, which gives

$$\dot{\epsilon}_p^{(k)} = \left(\frac{2\lambda}{3h}\right)\rho_d PT_f \times |Z_i^A D_i e^{-t'/\tau_i} - Z_v D_v (1 + S_k) e^{-t'/\tau_v}|. \quad (36)$$

Since interstitials diffuse much faster than vacancies, the creep rate equation can be separated into

$$\dot{\epsilon}_p^{(k)} = \left(\frac{2\lambda}{3h}\right)\rho_d PT_f \times \{Z_i^A D_i e^{-t'/\tau_i} - Z_v D_v (1 + S_k) e^{-t'/\tau_v}\} \quad (37)$$

$$T_{on} \leq t \leq T_0^k$$

and

$$\dot{\epsilon}_p^{(k)} = \left(\frac{2\lambda}{3h}\right)\rho_d PT_f \{Z_v D_v (1 + S_k) \times e^{-t'/\tau_v} - Z_i^A D_i e^{-t'/\tau_i}\} \quad T_0^k \leq t \leq T_f \quad (38)$$

where T_0^k is defined such that $V_c^k = 0$:

$$T_0^k = \frac{1}{(\lambda_i - \lambda_v)} \ln \left\{ \frac{Z_i^A D_i}{Z_v^0 (1 + S_k) D_v} \right\} + T_{on} \quad (39)$$

The total creep strain during the k th pulse is now obtained by integrating Eq. (37) between T_{on} and T_0^k , and Eq. (38) between T_0^k and T_f . Straightforward, but lengthy algebraic manipulations yield an expression for the creep strain that is given by:

$$\Delta \epsilon_p^{(k)} = \frac{2\lambda}{3h} \rho_d PT_f \{Z_i^A D_i \tau_i [1 + e^{-(T_f - T_{on})/\tau_i}] - 2e^{-(T_0^k - T_{on})/\tau_i} + Z_v^0 D_v \tau_v (1 + S_k)\} \times [2e^{-(T_0^k - T_{on})/\tau_v} - e^{-(T_f - T_{on})/\tau_v} - 1] \quad (40)$$

The magnitudes of the time constants are usually such that

$$\tau_i \ll T_0^k \ll \tau_v$$

and Eq. (40) simplifies to

$$\Delta \epsilon_p^{(k)} \approx \frac{2\lambda}{3h} PT_f \left\{ \frac{3Z_i^A}{(Z_i^A + 2Z_i^0)} + (1 - \tilde{\eta}_v)(1 + S_k) \right\} \quad (41)$$

Notice that for large k , the term $(1 - \tilde{\eta}_v)(1 + S_k)$ approaches unity, and the creep strain increment per pulse will be given by:

$$\Delta \epsilon_p^{(k)} |_{k \text{ large}} \approx \left(\frac{2\lambda}{3h}\right) PT_f \left\{ \frac{3Z_i^A}{(Z_i^A + 2Z_i^0)} + 1 \right\} \quad (42)$$

If we consider now the total creep strain, the contributions due to successive pulses have to be added. Therefore,

$$\epsilon_{\text{tot}}^{(N)} = \left(\frac{2\lambda}{3h} P T_f \right) \sum_{k=1}^N \left\{ \frac{3Z_i^A}{(Z_i^A + 2Z_i^0)} + (1 - \tilde{\eta}_v) \times \left(1 + \sum_{j=1}^{k-1} (\tilde{\eta}_v)^j \right) \right\} \quad (43)$$

After some straightforward algebra, Eq. (43) reduces to:

$$\epsilon_{\text{tot}}^{(N)} = \left(\frac{2\lambda}{3h} P T_f \right) N \left\{ \frac{3Z_i^A}{(Z_i^A + 2Z_i^0)} + (1 - \tilde{\eta}_v) \times \left[1 + \sum_{k=1}^{N-1} \left(1 - \frac{k}{N} \right) (\tilde{\eta}_v)^k \right] \right\} \quad (44)$$

Before examining the effects of point defect recombination, we will discuss the results of the calculations for the sink-dominant situation. A cold-worked first wall in ICFR's would contain a high initial dislocation density, corresponding to the conditions examined in this section.²² Calculations were performed for the parameters of stainless steel (see Table I) with a dislocation density of 10^{15} m/m³ and a period of $T_f = 0.2$ sec. First consider an average damage rate of $P = 10^{-6}$ dpa/s and temperatures ranging from 573 K to 723 K. For these parameters, the loss rate to sinks can be shown to be greater than the recombination rate throughout the entire period.

The validity of the approximate analytical expressions for C_v and C_i given by (32) and (33) was verified before calculating the resulting creep strain. The implicit multistep numerical integration methods of the GEAR computer package³¹ were utilized to evaluate C_v and C_i numerically. The analytical values agreed with the numerical results to within 3% for C_v and 23% for C_i after 100 pulses at 573 K. The larger error for C_i is attributed to the numerical integration, and does not affect the overall results because it occurs after the interstitial concentration has decreased by more than an order of magnitude.

Figure 12 illustrates the creep strain time behavior for damage-equivalent steady-irradiation and pulsed irradiation cases at 573 K. Since the vacancy mean life-time is approximately 5 sec., we observe a transient behavior in the pulsed creep strain which extends for a few vacancy mean life-times. Interstitials are quickly absorbed at dislocations during each pulse causing dislocations to climb over obstacles, and a strain increment is

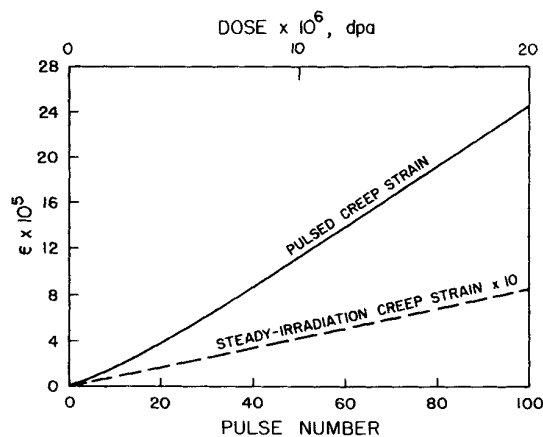


FIGURE 12 The creep strain as a function of time in an ICFR, neglecting recombination.

produced due to the almost instantaneous interstitial absorption. On the other hand, vacancies produced in one pulse diffuse on a much slower time scale to dislocations resulting in a climb in the opposite direction and another creep strain increment that is added to the interstitial contribution. During the first few pulses, however, the creep strain increment due to vacancies is relatively small resulting in the slow transient shown in Figure 12. Steady irradiation creep strain is also shown on the same figure. While the creep strain in the pulsed case is due to successive additions of vacancy and interstitial contributions, in the steady case it is determined by the difference between continuous interstitial and vacancy contributions. This explains the lower values of steady creep strain when compared to the equivalent pulsed creep strain. Under the assumptions and approximations used in the sink-dominant case, it can be shown that after a few vacancy mean lifetimes, the ratio of pulsed irradiation strain rate to the equivalent steady irradiation case ($\dot{\epsilon}^P/\dot{\epsilon}^S$) is given by (see Appendix B):

$$\left. \frac{\dot{\epsilon}^P}{\dot{\epsilon}^S} \right|_{t \gg \tau_v} = \frac{2Z_i^A + Z_i^0}{Z_i^A - Z_i^0} \quad (45)$$

When the period is longer than the vacancy mean lifetime, the creep strain will be linear with increasing pulse number, and the ratio of the creep strains will be the same as given by Eq. (45). In this particular case, we can write:

$$\left. \frac{\epsilon_c^P}{\epsilon_c^S} \right|_{T_f > \tau_v} \approx \left. \frac{\dot{\epsilon}^P}{\dot{\epsilon}^S} \right|_{t \gg \tau_v} \quad (46)$$

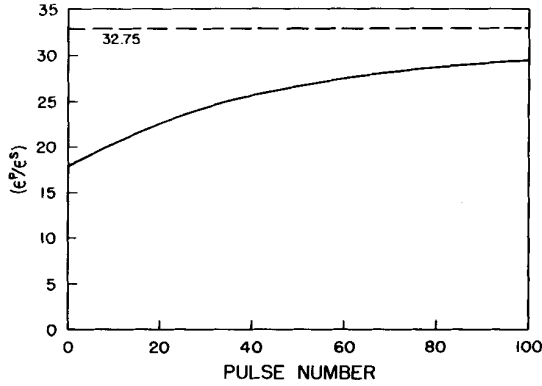


FIGURE 13 Ratio of pulsed to steady irradiation creep strain in an ICFR as a function of time, neglecting recombination.

The deviation from this ratio is attributed only to the transient behavior of vacancies. If we look back to Figure 12, we find that the ratio of the creep strains is not constant during the first few tens of pulses, but it tends to a constant value after long irradiation periods. While the ratio given by Eq. (45) is 32.75, it is smaller than this value for times less than $\sim 10\tau_v$. This is shown in Figure 13, where the ratio of pulsed irradiation creep strain to steady irradiation creep strain is plotted as a function of pulse number using Eq. (44). On the other hand, when $\tau_v < T_f$, the creep increment during the period T_f is independent of the irradiation time in both the pulsed and steady irradiation cases. It can also be shown from Eq. (41), and from a similar analysis of the steady irradiation case, that both $\Delta\epsilon_p^{(k)}$ and $\Delta\epsilon_{ss}$ are temperature-independent in the range of temperatures and irradiation conditions studied here. The creep strain increment during a 0.2 sec. period is 8.4×10^{-8} m/m for steady irradiation, while it is about 2.75×10^{-6} m/m for pulsed irradiation.

4b General Case of Point-Defect Kinetics Including Diffusion and Mutual Recombination

When the point defect generation rate is very high during the irradiation pulse, mutual recombination will also play an important role in determining point-defect fluxes. As discussed in the previous section, the on-time will be assumed to be shorter than τ_r and τ_i , such that both vacancies and interstitials achieve equal concentrations at the end of the pulse on-time. During this period, the concentrations are still described by Eqs. (29) and

(30). For times longer than T_{on} , on the other hand, Eq. (2) can be solved by setting $P = 0$ and $C_v \simeq C_i$ in the interstitial equation (see Ref. 30 for details).

Now define the dimensionless quantities $\tilde{\eta}_v$ and θ as:

$$\tilde{\eta}_v = \frac{C_v^{(1)}(T_f)}{PT_f} = e^{-(T_f - T_{on})/\tau_v}, \quad (47)$$

and

$$\theta = (\alpha PT_f \tau_i)^{-1} \quad (48)$$

Here, $\tilde{\eta}_v$ represents a dimensionless vacancy concentration at the end of the first T_f , had there been no recombination. θ is defined as the ratio of i -sink diffusion rate to recombination rate at the end of the first T_{on} . Following the solutions developed by Ghoniem and Gurol,³⁰ the point defect concentrations at any time t measured from the start of the off-time of the k th pulse are given by:

$$C_v^{(k)}(t) = \left\{ \frac{(1 + \eta^{(k)})(\theta + \eta^{(k)})}{1 + \theta + \eta^{(k)} - e^{-(t - T_{on})/\tau_i^{(k)}}} \right\} \times PT_f e^{-(t - T_{on})/\tau_v} \quad (49)$$

$$C_i^{(k)}(t) = \left\{ \frac{(\theta + \eta^{(k)})}{1 + \theta + \eta^{(k)} - e^{-(t - T_{on})/\tau_i^{(k)}}} \right\} \times PT_f e^{-(t - T_{on})/\tau_i^{(k)}} \quad (50)$$

where $\eta^{(k)}$ is determined from the recurrence formula

$$\eta^{(k)} = \frac{(\theta + \eta^{(k-1)})(1 + \eta^{(k-1)})\tilde{\eta}_v}{(1 + \theta + \eta^{(k-1)})}, \quad k \geq 2 \quad (51)$$

$$\eta^{(1)} = 0, \quad (52)$$

and the interstitial mean lifetime during the k th pulse, $\tau_i^{(k)}$, is determined by

$$\tau_i^{(k)} = \tau_i \left[1 + \frac{\eta^{(k)}}{\theta} \right]^{-1}, \quad k \geq 1 \quad (53)$$

In order to evaluate the creep strain during the k th pulse, we will separate the creep rate Eq. (1) into two parts. Here, we follow a similar procedure to that of the last section. For times $T_{on} \leq t \leq T_0^{(k)}$, the major contribution to the creep strain results from the interstitial flux, while vacancies take over for $t > T_0^{(k)}$. The time $T_0^{(k)}$ is defined as the time at which the dislocation climb velocity becomes zero during the k th pulse. This is given by

$$T_0^{(k)} = \frac{\tau_i^{(k)}\tau_v}{(\tau_v - \tau_i^{(k)})} \ln \left\{ \frac{Z_i^A D_i}{Z_v^0 D_v (1 + \eta^{(k)})} \right\} + T_{on} \quad (54)$$

TABLE III

A comparison between analytically and numerically evaluated vacancy concentrations after 100 pulses.

Temperature, K	Numerical C_v (at/at)	Analytical C_v (at/at)	% Error
573	6.158×10^{-5}	6.030×10^{-5}	2.07
673	1.163×10^{-6}	1.231×10^{-6}	5.50

The total creep strain during the k th pulse can be shown to be given by (see Appendix E):

$$\Delta \epsilon_p^{(k)} = \left(\frac{2 \lambda}{3 h} \right) P T_f (\theta + \eta^{(k)}) \left\{ \frac{Z_i^A \theta}{Z_i^0 D_v (\theta + \eta^{(k)})} \times \ln \left[\frac{1 + \theta + \eta^{(k)}}{\theta + \eta^{(k)}} \right] + \frac{(1 + \eta^{(k)})(1 - \tilde{\eta}_v)}{(1 + \theta + \eta^{(k)})} \right\} \quad (55)$$

In the special case when sink diffusion dominates over recombination, θ becomes much larger than 1, and $\eta^{(k)}$ becomes very small. The last equation can then be shown to resort to the simpler expression given by (41) in the previous section. The total creep strain after many pulses is obtained by summing the contributions of the individual pulses.

A numerical integration was performed using the GEAR computer package³² to test the validity of Eqs. (49) and (50) that describe point defect concentrations during any pulse k . At an average displacement rate of 10^{-4} dpa/sec., pulse period of 0.2 sec. and a dislocation density of 10^{15} m/m³, the results of Table III were obtained at the end of 100 pulses.

The results of the calculations clearly indicate the high accuracy of Eqs. (49) and (50) when used for irradiation creep studies.

The high displacement rate results are given in Table IV for stainless steel with an average displacement rate of 10^{-4} dpa/sec. and a dislocation density of 10^{15} m/m³. The high damage rate was considered for the following reasons: (a) A high displacement rate will allow the effects of mutual

recombination to be analyzed, and compared to the same case without recombination; (b) A damage rate of 10^{-4} dpa/sec. corresponds to the surface conditions of ICFR's;²² (c) Such a damage rate can be easily achieved in simulation facilities.

Under steady irradiation, and when the sink strength is independent of irradiation temperature, the role of recombination diminishes as the temperature increases.³⁵ Thus, the fraction of point defects absorbed at dislocations increases at higher temperatures, thereby enhancing irradiation creep by the climb-glide mechanism. This behavior is clearly shown in Table IV, where the steady-irradiation creep strain increases up to saturation (around 800 K). On the other hand, the effects of recombination during pulsed irradiation of the ICFR type can be understood in terms of two simple quantities: θ and $\tilde{\eta}_v$. First, θ is an indication of the amount of recombination during one pulse. This is almost temperature independent. And second, $\tilde{\eta}_v$ gives the magnitude of vacancy overlap from one pulse to the next. $\tilde{\eta}_v$ is large (close to unity) at low temperature and approaches zero as the temperature increases. The lower temperatures are characterized by a high degree of overlap ($\tilde{\eta}_v \approx 1$), and interpulse recombination plays a significant role in decreasing the creep rate. As the temperature increases, point defect recombination due to pulse overlap becomes insignificant, and the only effect is due to recombination within each pulse. The ratio of pulsed to steady-irradiation creep drops down to ~ 15 at high temperatures. One should observe here that this less than one-

TABLE IV

Irradiation creep results for the ICFR after 1000 pulses
($P = 10^{-4}$ dpa/sec., $T_f = 0.25$ sec., $\rho_d = 10^{15}$ m⁻²)

Temperature, K	ϵ_s (m/m)	ϵ_p (m/m)	Ratio (ϵ_p/ϵ_s)	$\tilde{\eta}_v$	θ
573	1.09×10^{-3}	0.0345	31.56	0.9639	0.5292
623	2.76×10^{-3}	0.0788	28.57	0.7377	0.5292
673	5.15×10^{-3}	0.1209	23.48	0.1590	0.5292
723	7.09×10^{-3}	0.1283	18.10	1.724×10^{-4}	0.5292
773	7.97×10^{-3}	0.1283	16.10	3.067×10^{-15}	0.5292
873	8.35×10^{-3}	0.1283	15.37	1.929×10^{-22}	0.5292

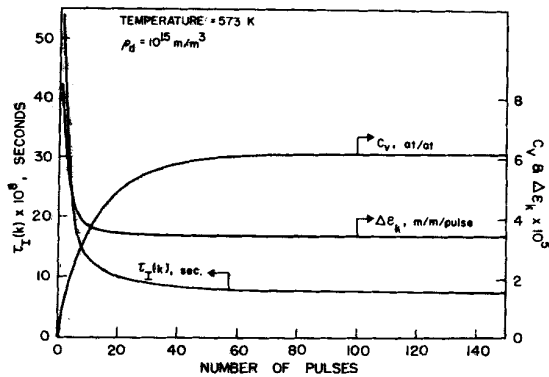


FIGURE 14 The effective interstitial mean lifetime $\tau_i^{(k)}$, incremental creep $\Delta\epsilon_k$, and the vacancy concentrations vs. the number of pulses under ICFR conditions, including recombination.

half the corresponding ratio at $P = 10^{-6}$ dpa/sec. where point defect recombination is negligible altogether. This shows that the high average displacement rate is accompanied by a smaller fraction of surviving point defects, and hence a lower creep rate.

Figure 14 shows $\tau_i^{(k)}$, $\Delta\epsilon_k$ and the vacancy concentration at the end of each pulse at a temperature of 573 K and $\rho_d = 10^{15}$ m/m³. The effective interstitial mean life-time ($\tau_i^{(k)}$) decreases sharply from 0.5 μ sec. to 0.08 μ sec. in about 50 pulses. The vacancy concentration, on the other hand, increases from pulse to pulse until it reaches steady-state (repeatable profiles from one pulse to the next)

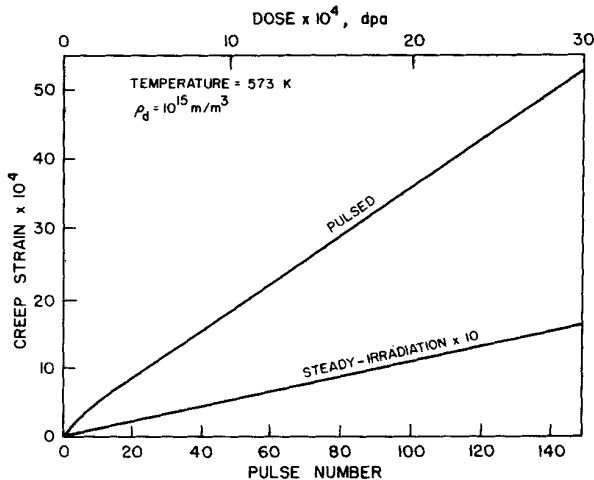


FIGURE 15 The creep strain as a function of time in an ICFR, including recombination.

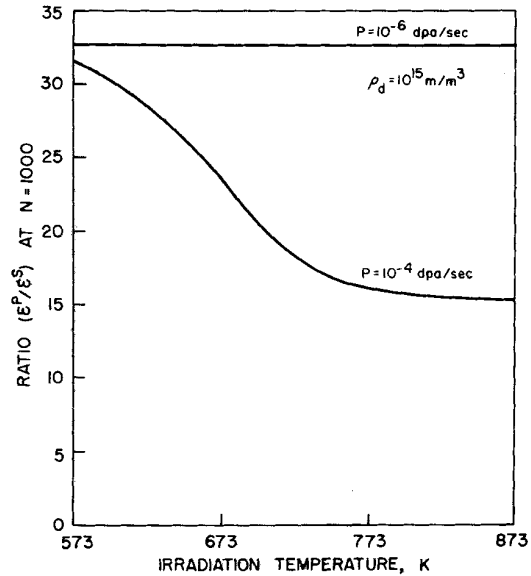


FIGURE 16 Ratio of pulsed to steady irradiation creep strain in an ICFR as a function of temperature after 1000 pulses, including recombination.

after about 50 pulses. The net effect is a sharply decreasing transient in the creep strain increment ($\Delta\epsilon_k$), that levels off approximately after the same number of pulses. It is interesting to note that this transient behavior is strongly related to the vacancy mean life-time, which is approximately 5 sec. in this case. The results of the calculations for the pulsed and steady-irradiation total creep strain are shown in Figure 15. While the pulsed creep starts with a transient due to the rapid decline in $\Delta\epsilon_k$, the steady-irradiation equivalent shows a linear dose dependence. Irradiation pulsing shows an enhancement of the creep strain of over a factor of 30. The ratio of pulsed to steady-irradiation creep strain as a function of temperature after 1000 pulses is shown in Figure 16. As has been previously discussed, point defect recombination loses its importance for steady-irradiation at high temperatures, while it reduces the fraction going to dislocations at all temperatures for pulsed irradiation. The ratio (ϵ^P/ϵ^S), therefore, declines to ~ 15 at the high temperatures as shown in the figure.

5 CONCLUSIONS

This paper has dealt with the effects of radiation pulsing on the climb-controlled glide creep strain

in fusion systems. Throughout, the rate theory formulation has been used to describe the point-defect kinetics and the sink densities have been assumed to be temperature-independent. The major conclusions can be summarized as follows:

5a TOKAMAKS

In the sink-dominant case the creep strain can be evaluated analytically within the framework of the rate theory. For a NUWMAK type fusion reactor operating approximately in the temperature range $T > 715$ K, the creep increases linearly as a function of the number of pulses. The pulsed creep is found to be about the same as the steady irradiation creep. Furthermore, the creep is insensitive to temperature (when ρ_d is assumed to be temperature-independent).

When recombination is included, one must resort to modeling the point-defect kinetics in order to calculate the creep. For the case where the vacancies never reach their steady state concentration in the total observation time (i.e. $\tau_v > NT_f$), the pulsed creep is always somewhat greater than the steady irradiation creep, and the small difference between them increases with temperature. It is the additive contribution of the vacancy flux during the pulse off-time which gives rise to the enhanced creep under pulsing. Decreasing the temperature decreases the off-time creep. When the temperature is low enough so that $\tau_v \approx 4NT_f$, the creep becomes temperature-independent and is dictated by the interstitial flux.

The case where vacancies reach their steady-state concentrations during a single pulse ($\tau_v < T_{on}$) was also considered. Again the recombination is included by modeling the point-defect kinetics. For this case, it is found that the creep is a linear function of the number of pulses. Corresponding to $\tau_v < T_{on}$, we have investigated the creep of 316SS in a NUWMAK type reactor for $T = 572$ K and $T = 557$ K ($\tau_v = 0.2T_{on}$ and $\tau_v = 0.4T_{on}$ respectively). A creep enhancement of about two to three is found under these conditions.

5b Pulsed Accelerators

The creep strain was investigated for an accelerator with on-time of 0.23 sec. and off-time of 0.015 sec. for $T > 715$ K, corresponding to the sink-dominant regime. The parameters were chosen to represent an experimental scaled down simulation of the NUWMAK design. Since $\tau_v \gg T_f$, there

will be overlapping of the vacancy concentrations from previous pulses. This overlap produces a strain transient which extends for 20–30 pulses at 715 K, giving rise to a large strain rate during this transient. As the irradiation temperature increases the transient becomes less pronounced, with a lower creep rate in the linear regime.

Using the numerical values for nickel given in Table I, we have compared our theoretical results (including recombination) with the pulsed accelerator experiment of Simonen and Hendrick,¹⁷ who used an on-time of 1000 sec., followed by 100 sec. annealing. Our results compare favorably, giving rise to about a three-fold enhancement over steady irradiation, and reproducing the correct magnitude of the measured creep. However, since the numerical values used have uncertainties, it can only be claimed that the physics of the pulsed creep model we have presented (for $\tau_v < T_{on}$) correctly reproduces the experimental results for the numerical values used.

5c Inertial Confinement Fusion Reactors

In the sink-dominant case corresponding to low average damage rates ($\sim 10^{-6}$ dpa/sec.), it is found that after an initial transient, the ratio of the pulsed to steady irradiation creep approaches the constant, temperature-independent value given by Eq. (45), which depends only on the point-defect bias factors. With the bias factors used in our calculations this ratio is about 33. When the point-defect generation rate is very high, corresponding to the surface conditions of ICFR's, mutual recombination plays an important role in determining the point-defect fluxes, and hence the resulting creep strain. When the point-defect recombination is important, it is found that the creep enhancement due to pulsing is temperature-dependent. For conditions typical of ICFR first walls ($P = 10^{-4}$ dpa/sec., $T_f = 0.25$ sec., $\rho_d = 10^{15}$ m⁻²) after 1000 pulses, it is found that the ratio of pulsed to steady irradiation creep has a value of about 32 on the low temperature end of 573 K. The low temperature end is characterized by a high degree of vacancy overlap, and recombination due to this overlap plays a significant role in determining the pulsed creep strain. The ratio of pulsed to steady irradiation creep decreases as the temperature is increased, and saturates to a value of about 15 near $T = 873$ K.

As mentioned in the introduction, the point-defect concentration fluctuations due to ran-

domly produced cascades are expected to significantly influence the creep under ICFR conditions. Since we have used the rate theory formulation in this study, our results represent an upper bound for true pulsed creep. Inclusion of the fluctuations is expected to give rise to pulsed creep that is between that predicted here and the steady irradiation creep.

5d General Remarks

In all the systems that have been studied, it has been shown that the mean vacancy diffusion time to sinks, τ_v , plays a very central role in determining the amount of creep enhancement to be expected due to pulsing. Furthermore, maintaining equal average damage rates, the enhancement will be greater for the system with the greater percentage off-time.

ACKNOWLEDGEMENTS

We are grateful for the support provided by the National Science Foundation through Grant Nos. ENG 78-05554 and ENG 78-05413, and also the support of the College of Engineering, UCSB and the School of Engineering and Applied Science, UCLA.

REFERENCES

1. W. G. Wolfer and J. L. Straalsund, *Scripta Met.*, **7**, 161 (1973).
2. W. G. Wolfer, *Scripta Met.*, **9**, 801 (1975).
3. R. Bullough and M. R. Hayns, *J. Nucl. Mat.*, **57**, 348 (1975).
4. E. R. Gilbert and J. F. Bates, *J. Nucl. Mat.*, **65**, 204 (1977).
5. E. R. Gilbert, J. L. Straalsund, and G. L. Wire, *J. Nucl. Mat.*, **65**, 266 (1977).
6. R. Bullough and M. R. Hayns, *J. Nucl. Mat.*, **65**, 184 (1977).
7. H. R. Brager, *et al.*, Stress-affected microstructural development and creep-swelling inter-relationships, *Proc. of Conf. on Radiation Effects in Breeder Reactor Structural Materials*, June 19-23 (1977), 727.
8. D. J. Michel, P. L. Hendrick, and A. G. Pieper, *J. Nucl. Mat.*, **75**, 1 (1978).
9. E. K. Opperman, *et al.*, *Nucl. Technology*, **42**, 71 (1979).
10. L. K. Mansur, *Phil. Mag. A*, **39**, No. 4, 497 (1979).
11. M. H. Woo, *J. Nucl. Mat.*, **80**, 132 (1979).
12. F. V. Nolfi, Jr., *et al.*, *Scripta Met.*, **13**, 231 (1979).
13. R. Bullough and M. H. Wood, Mechanisms of radiation induced creep and growth, Harwell Report, TP 797 (1979).
14. F. A. Nichols, *J. Nucl. Mat.*, **84**, 207 (1979).
15. W. J. Duffin and F. A. Nichols, *J. Nucl. Mat.*, **45**, 302 (1972/73).
16. MacEwen and Fidleris, *Phil. Mag.*, **31**, 1149 (1975).
17. E. P. Simonen and P. L. Hendrick, Light ion irradiation-induced creep mechanisms in nickel, *Proc. of Conf. on Fusion Reactor Material*, 29-31 Jan., 1979, Miami Beach, Fl.
18. R. R. Vandervoort, W. L. Barmore, and A. K. Mukherjee, *Rad. Eff.*, **41**, 113 (1979).
19. P. T. Heald and M. V. Speight, *Phil. Mag.*, **29**, 1075 (1974).
20. R. Bullough and J. R. Willis, *Phil. Mag.*, **31**, 855 (1975).
21. W. G. Wolfer and M. Ashkin, *J. Appl. Phys.*, **46**, 547 (1975).
22. N. M. Ghoniem and G. L. Kulcinski, A critical assessment of the effects of pulsed irradiation on materials, *Univ. of Wisconsin Fusion Report UWFD-311*.
23. E. P. Simonen, Radiation creep in transient irradiation environments, *Proc. of Int. Conf. on Fundamental Mechanisms of Radiation-Induced Creep and Growth*, Chalk River, Ont., Canada, May (1979).
24. R. Sizmann, *J. Nucl. Mater.*, **69/70**, 386 (1978).
25. C. Abromeit and R. Poerschke, *J. Nucl. Mater.*, **82**, 298 (1979).
26. B. Badger, *et al.*, NUWMAK: A Tokamak reactor design study, *Univ. of Wisconsin Fusion Report, UWFD-330* (1979).
27. N. M. Ghoniem and G. L. Kulcinski, *J. Nucl. Mater.*, **85/86**, 547 (1978).
28. L. K. Mansur, W. A. Coghlan, and A. D. Brailsford, Swelling with inhomogeneous point defect production—A cascade diffusion theory, Ref. 17 above.
29. N. M. Ghoniem and G. L. Kulcinski, *Rad. Eff.*, **41**, 81 (1979).
30. N. M. Ghoniem and H. Gurol, An analytical approach to void growth in inertial confinement fusion reactor first walls, *Univ. of California Eng. Report, UCLA-ENG-7984* (1979), to be published.
31. M. H. Yoo, *J. Nucl. Mat.*, **68**, 193 (1977).
32. A. C. Hindmarch, *Lawrence Livermore Lab. Report, UCID-30001*, Rev. 3, (1974).
33. A. Z. Akcasu and H. Gurol, *J. Polymer Science (Physics Ed.)*, **14**, 1 (1976).
34. J. A. Sprague and S. A. Smidt, Jr., NRL Memorandum Report 2629 (1973).
35. H. Wiedersich, *Rad. Eff.*, **12**, 111 (1972).

Appendix A

DERIVATION OF THE PULSED CREEP STRAIN FOR THE SINK-DOMINANT CASE

Neglecting recombination, the point-defect concentrations are given by

$$\frac{dC_i}{dt} = P - \lambda_i C_i \quad (\text{A.1})$$

$$\frac{dC_v}{dt} = P - \lambda_v C_v$$

During the *on-time* of the first pulse, the vacancy and interstitial concentrations become (using $C_i(0) = C_v(0) = 0$)

$$\begin{aligned} C_v^{(1)}(t) &= \frac{P}{\lambda_v} (1 - e^{-\lambda_v t}) \\ C_i^{(1)}(t) &= \frac{P}{\lambda_i} (1 - e^{-\lambda_i t}) \end{aligned} \quad (\text{A.2})$$

In general, the vacancies may not have reached their steady-state value of P/λ_v , but the interstitials will have (during the *on-time*), therefore the concentrations during the *off-time* of pulse 1 are

$$\begin{aligned} C_v^{(1)}(t) &= \frac{P}{\lambda_v} (1 - e^{-\lambda_v T_{\text{on}}}) e^{-\lambda_v(t - T_{\text{on}})} \\ C_i^{(1)}(t) &= \frac{P}{\lambda_i} e^{-\lambda_i(t - T_{\text{on}})} \end{aligned} \quad (\text{A.3})$$

When the second pulse is turned on, the vacancies start increasing from where they left off at the end of pulse one. On the other hand, the interstitials repeat the behavior of pulse one. Hence, during the *on-time* of pulse 2, $C_v^{(2)}(t)$ and $C_i^{(2)}(t)$ become (from Eq. A.1)

$$\begin{aligned} C_v^{(2)}(t) &= \frac{P}{\lambda_v} (1 - e^{-\lambda_v T_{\text{on}}}) e^{-\lambda_v(t - T_{\text{on}})} \\ &\quad + \frac{P}{\lambda_v} (1 - e^{-\lambda_v(t - T_{\text{r}})}) \\ C_i^{(2)}(t) &= \frac{P}{\lambda_i} (1 - e^{-\lambda_i(t - T_{\text{r}})}) \end{aligned} \quad (\text{A.4})$$

During the *off-time* vacancies from the first pulse might still be diffusing to sinks, therefore during the *off-time* of pulse 2 we get

$$\begin{aligned} C_v^{(2)}(t) &= \frac{P}{\lambda_v} (1 - e^{-\lambda_v T_{\text{on}}}) e^{-\lambda_v(t - T_{\text{on}})} \\ &\quad + \frac{P}{\lambda_v} (1 - e^{-\lambda_v T_{\text{on}}}) e^{-\lambda_v(t - [T_{\text{r}} + T_{\text{on}}])} \\ C_i^{(2)}(t) &= \frac{P}{\lambda_i} e^{-\lambda_i(t - [T_{\text{r}} + T_{\text{on}}])} \end{aligned} \quad (\text{A.5})$$

Continuing in this manner gives Eqs. (5a) and (5b), and Eq. (6) from Section 2, for the k th pulse. Here we have used the fact that since λ_i is very large ($\sim 10^8/\text{sec.}$), the interstitials reach their steady-state concentration almost instantaneously during the *on-time*, and will also rapidly go to the equilibrium concentration when the pulse is turned off.

The creep rate during the k th pulse is then given by Eqs. (7a) and (7b). The creep strain increment during the k th pulse is given by

$$\Delta \varepsilon_p^{(k)} = \int_{\text{on-time}} \dot{\varepsilon}_p^{(k)}(t) dt + \int_{\text{off-time}} \dot{\varepsilon}_p^{(k)}(t) dt \quad (\text{A.6})$$

The result becomes

$$\begin{aligned} \Delta \varepsilon_p^{(k)} &= \left(\frac{2}{3} \frac{\lambda}{h} P \right) \left\{ \left[\frac{Z_i^A \rho_d}{Z_i^A \rho_d^A + Z_i^0 \rho_d^N} - 1 \right] T_{\text{on}} \right. \\ &\quad + \tau_v (1 - e^{-\lambda_v T_{\text{on}}}) \left[1 - (e^{\lambda_v T_{\text{on}}} - 1) e^{-\lambda_v(k-1)T_{\text{r}}} \right. \\ &\quad \times \left. \sum_{j=0}^{k-2} e^{j\lambda_v T_{\text{r}}} \right] + \tau_v [e^{\lambda_v(T_{\text{r}} - T_{\text{on}})} - 1] \\ &\quad \times \left. e^{-\lambda_v k T_{\text{r}}} (e^{\lambda_v T_{\text{on}}} - 1) \sum_{j=0}^{k-1} e^{j\lambda_v T_{\text{r}}} \right\} \end{aligned} \quad (\text{A.7})$$

The total creep at the end of N pulses is then given by

$$\varepsilon_p^{(N)} = \sum_{k=1}^N \Delta \varepsilon_p^{(k)} \quad (\text{A.8})$$

Using Eq. (A.7), $\varepsilon_p^{(N)}$ becomes

$$\begin{aligned} \varepsilon_p^{(N)} &= \left(\frac{2}{3} \frac{\lambda}{h} P \right) \left\{ \left[\frac{Z_i^A \rho_d}{Z_i^A \rho_d^A + Z_i^0 \rho_d^N} - 1 \right] N T_{\text{on}} \right. \\ &\quad + \tau_v (1 - e^{-\lambda_v T_{\text{on}}}) \left[N - e^{\lambda_v T_{\text{r}}} (e^{\lambda_v T_{\text{on}}} - 1) \right. \\ &\quad \times \sum_{k=2}^N \sum_{j=0}^{k-2} e^{\lambda_v(j-k)T_{\text{r}}} \left. \right] + \tau_v (e^{\lambda_v(T_{\text{r}} - T_{\text{on}})} - 1) \\ &\quad \times \left. (e^{\lambda_v T_{\text{on}}} - 1) \sum_{k=2}^N \sum_{j=0}^{k-1} e^{\lambda_v(j-k)T_{\text{r}}} \right\} \end{aligned} \quad (\text{A.9})$$

Double sums involving difference of two indices also occurs in studying polymer molecule dynamics. It can easily be shown³³ that

$$\sum_{k=2}^N \sum_{j=0}^{k-2} e^{-\lambda_v(k-j)T_{\text{r}}} = \sum_{k=2}^N (N+1-k) e^{-\lambda_v k T_{\text{r}}} \quad (\text{A.10})$$

and

$$\sum_{k=2}^N \sum_{j=0}^{k-1} e^{-\lambda_v(k-j)T_{\text{r}}} = \sum_{k=1}^N (N+1-k) e^{-\lambda_v k T_{\text{r}}}$$

Using these in Eq. (A.9) gives Eq. (10) in the text.

Appendix B

CALCULATION OF THE STEADY IRRADIATION CREEP FOR THE SINK-DOMINANT CASE

Under steady irradiation, the creep rate is

$$\dot{\epsilon}_s = \left(\frac{2\lambda}{3h} \rho_d \right) |Z_i^A D_i C_i^{ss} - Z_v^0 D_v C_v^{ss}| \quad (\text{B.1})$$

Here we assume that the initial transient in the point-defect kinetics is over and the vacancies and interstitials have reached their steady-state values, that is

$$\begin{aligned} C_i^{ss} &= \frac{P}{\lambda_i} \\ C_v^{ss} &= \frac{P}{\lambda_v} \end{aligned} \quad (\text{B.2})$$

where

$$\begin{aligned} \lambda_i &= (Z_i^A \rho_d^A + Z_i^0 \rho_d^N) D_i \\ \lambda_v &= Z_v^0 D_v \rho_d \end{aligned} \quad (\text{B.3})$$

Using these in Eq. (B.2), we get

$$\dot{\epsilon}_s = \left(\frac{2\lambda}{3h} P \right) \left| Z_i^A D_i \frac{\rho_d}{\lambda_i} - 1 \right| \quad (\text{B.4})$$

Since the interstitial flux is always somewhat greater than the vacancy flux in steady-state, and using (B.3), this equation becomes

$$\dot{\epsilon}_s = \left(\frac{2\lambda}{3h} P \right) \left\{ \frac{Z_i^A \rho_d}{Z_i^A \rho_d^A + Z_i^0 \rho_d^N} - 1 \right\} \quad (\text{B.5})$$

Assuming that one-third of the dislocations are aligned we get

$$\dot{\epsilon}_s = \left(\frac{4\lambda}{3h} P \right) \left\{ \frac{Z_i^A - Z_i^0}{Z_i^A + 2Z_i^0} \right\}. \quad (\text{B.6})$$

Appendix C

PULSED CREEP INCLUDING RECOMBINATION FOR THE CASE

$$\tau_v > NT_f$$

From Eqs. (16a) and (16b), the creep increment for the k th pulse can be evaluated as (see Eq. 8)

$$\begin{aligned} \Delta\epsilon_p^{(k)}(t) &= \left(\frac{2\lambda}{3h} \rho_d \right) \left\{ Z_i^A D_i \left(\frac{P}{\alpha\lambda_i} \right)^{1/2} 2T_{on}^{1/2} \right. \\ &\quad \times [k^{1/2} - (k-1)^{1/2}] - Z_v^0 D_v \left(\frac{P\lambda_i}{\alpha} \right)^{1/2} \frac{2}{3} T_{on}^{3/2} \\ &\quad \times [k^{3/2} - (k-1)^{3/2}] + Z_v^0 D_v \left(\frac{P\lambda_i}{\alpha} \right)^{1/2} \\ &\quad \left. \times T_{on}^{1/2} k^{1/2} (T_f - T_{on}) \right\} \end{aligned} \quad (\text{C.1})$$

which is valid for $k \geq 2$. The total creep at the end

of N pulses is then given by

$$\epsilon_p^{(N)} = \Delta\epsilon_p^{(1)} + \sum_{k=2}^N \Delta\epsilon_p^{(k)} \quad (\text{C.2})$$

$$\begin{aligned} \epsilon_p^{(N)} &= \Delta\epsilon_p^{(1)} + \left(\frac{2\lambda}{3h} \rho_d \right) \left\{ 2Z_i^A D_i \left(\frac{PT_{on}}{\alpha\lambda_i} \right)^{1/2} \right. \\ &\quad \sum_{k=2}^N [k^{1/2} - (k-1)^{1/2}] - Z_v^0 D_v \left(\frac{P\lambda_i T_{on}}{\alpha} \right)^{1/2} \\ &\quad \times \left[\frac{2}{3} T_{on} \sum_{k=2}^N [k^{3/2} - (k-1)^{3/2}] \right. \\ &\quad \left. \left. - (T_f - T_{on}) \sum_{k=2}^N k^{1/2} \right] \right\}. \end{aligned} \quad (\text{C.3})$$

Now note

$$\begin{aligned} \sum_{k=2}^N [k^{1/2} - (k-1)^{1/2}] &= \sum_{k=2}^N k^{1/2} \\ - \sum_{k=1}^{N-1} k^{1/2} &= N^{1/2} - 1 \end{aligned}$$

and

$$\sum_{k=2}^N [k^{3/2} - (k-1)^{3/2}] = N^{3/2} - 1 \quad (\text{C.4})$$

We also approximate the summation of $k^{1/2}$ by an integral

$$\sum_{k=2}^N k^{1/2} \approx \int_1^N dx x^{1/2} = \frac{2}{3}[N^{3/2} - 1] \quad (\text{C.5})$$

This approximation becomes more accurate as N increases. For example, for $N = 10$ it is accurate to within $\sim 5\%$. Using (C.4) and (C.5) in Eq. (C.3) gives the result, Eq. (18) in Section 3. The creep contributions of the on- and off-times can be obtained by using Eq. (16a) to calculate $\epsilon_{\text{on}}^{(k)}$ and (16b) to calculate $\Delta \epsilon_{\text{off}}^{(k)}$, where the respective intervals are integrated over. Performing the summation (as in (C.2)) gives Eqs. (19) and (20).

During the first pulse, the point-defect behavior is different from later pulses, as seen in Figure 2.

Since τ_i is a very short time, C_v and C_i can be assumed to start from P/λ_i initially. Therefore, during the first pulse there are three regions to consider. The creep rate in these respective regions is given by:

$$\dot{\epsilon}_p^{(1)} = \left(\frac{2}{3} \frac{\lambda}{h} \rho_d\right) \left\{ Z_i^A D_i \frac{P}{\lambda_i} - Z_v^0 D_v P t \right\}, \quad 0 \leq t \leq \tau_r \quad (\text{C.6})$$

$$\dot{\epsilon}_p^{(1)} = \left(\frac{2}{3} \frac{\lambda}{h} \rho_d\right) \left\{ Z_i^A D_i \left(\frac{P}{\alpha \lambda_i}\right)^{1/2} t^{-1/2} - Z_v^0 D_v \left(\frac{P \lambda_i}{\alpha}\right)^{1/2} t^{1/2} \right\}, \quad t_r \leq t \leq T_{\text{on}} \quad (\text{C.7})$$

$$\dot{\epsilon}_p^{(1)} = \left(\frac{2}{3} \frac{\lambda}{h} \rho_d\right) Z_v^0 D_v \left(\frac{P \lambda_i}{\alpha}\right)^{1/2} T_{\text{on}}^{1/2}, \quad T_{\text{on}} \leq t \leq T_f$$

Integrating the above rates over their time intervals, gives $\Delta \epsilon_p^{(1)}$ given by Eq. (18b).

Appendix D

CALCULATION OF t^* (FOR $\tau_v < T_{\text{on}}$)

The time t^* can be obtained by equating the concentration at the end of pulse one, $C_v^{(1)}(T_f)$, with the concentration at time t^* obtained by the dashed line in Figure 9. That is

$$C_v^{(1)}(T_f) = C_v^{(1)}(t^*)$$

or

$$C_v^{(1)}(\tau_v) e^{-\lambda_v(T_f - T_{\text{on}})} = \left(\frac{P \lambda_i}{\alpha}\right)^{1/2} (t^*)^{1/2}. \quad (\text{D.1})$$

Using the value of $C_v^{(1)}(\tau_v)$, we get

$$(t^*)^{1/2} = (\tau_v)^{1/2} e^{-\lambda_v(T_f - T_{\text{on}})}, \quad (\text{D.2})$$

or $t^* = f \tau_v$,

$$f \equiv \exp[-2\lambda_v(T_f - T_{\text{on}})]$$

Appendix E

DERIVATION OF THE ICFR CREEP STRAIN IN THE GENERAL CASE

The point defect concentration during the k th pulse can be written as

$$C_v^{(k)}(x) = \frac{A e^{-x}}{B - e^{-ax}}, \quad x \geq 0 \quad (\text{E.1})$$

$$C_i^{(k)}(x) = \frac{D e^{-ax}}{B - e^{-ax}}, \quad x \geq 0 \quad (\text{E.2})$$

where,

$$\begin{aligned} A &= (1 + \eta^{(k)})(\theta + \eta^{(k-1)}) P T_f, \\ B &= (1 + \theta + \eta^{(k-1)}) P T_f, \\ F &= (\theta + \eta^{(k-1)}) P T_f, \end{aligned} \quad (\text{E.3})$$

$$x = (t - T_{\text{on}})/\tau_v,$$

and

$$a = \tau_v/\tau_i^{(k)} \gg 1.$$

In the first part of the cycle, interstitials will cause the dislocation to move in a certain direction. Then the arrival of vacancies reverses the direction of motion. The time, $T_0^{(k)}$, at which the dislocation motion is temporarily halted, is determined by setting the net point defect flux equal to zero.

$$Z_i^A D_i C_i^{(k)} = Z_v^0 D_v C_v^{(k)}$$

which yields,

$$T_0^{(k)} = \frac{\tau_v \tau_i^{(k)}}{\tau_v - \tau_i^{(k)}} \ln \left\{ \frac{Z_i^A D_i}{Z_v^0 D_v (1 + \eta^{(k)})} \right\} + T_{on} \quad (E.4)$$

Noting that $\tau_i^{(k)} \ll T_0^{(k)} \ll \tau_v$, an excellent approximation to the creep strain increment during the k th pulse is obtained by integrating the interstitial contribution between T_{on} and $T_0^{(k)}$, the vacancy contribution between $T_0^{(k)}$ and T_f , and neglecting the creep strain during the on-time. Thus,

$$\begin{aligned} \Delta \varepsilon_p^{(k)} &= \int_0^{T_f} \dot{\varepsilon}_p^{(k)} dt = \left(\frac{2\lambda}{3h} \right) \rho_d \tau_v \left\{ Z_i^A D_i \int_{t=T_{on}}^{t=T_0^{(k)}} \frac{F e^{-ax} dx}{B - e^{-ax}} \right. \\ &\quad \left. + Z_v^0 D_v \int_{t=T_0^{(k)}}^{t=T_f} \frac{A e^{-x} dx}{B - e^{-ax}} \right\} \quad (E.5) \\ &= \left(\frac{2\lambda}{3h} \right) \rho_d P T_f \left\{ Z_i^A D_i \tau_i^{(k)} (\theta + \eta^{(k)}) \right. \\ &\quad \left. \times \ln \left[\frac{1 + \theta + \eta^{(k)} - e^{-(T_0^{(k)} - T_{on})/\tau_i^{(k)}}}{\theta + \eta^{(k)}} \right] \right. \\ &\quad \left. + \frac{Z_v^0 D_v \tau_v (\theta + \eta^{(k)}) (1 + \eta^{(k)}) (e^{-(T_0^{(k)} - T_{on})/\tau_v} - \tilde{\eta}_v)}{(1 + \theta + \eta^{(k)})} \right\} \quad (E.6) \end{aligned}$$

The last expression can be approximated further by noting that $e^{-(T_0^{(k)} - T_{on})/\tau_i} \approx 0$, and that $e^{-(T_0^{(k)} - T_{on})/\tau_v} \approx 1$. Therefore,

$$\begin{aligned} \Delta \varepsilon_p^{(k)} &= \left(\frac{2\lambda}{3h} \right) P T_f (\theta + \eta^{(k)}) \left\{ \frac{Z_i^A \theta}{Z_i^0 (\theta + \eta^{(k)})} \right. \\ &\quad \left. \times \ln \left[\frac{1 + \theta + \eta^{(k)}}{\theta + \eta^{(k)}} \right] + \frac{(1 + \eta^{(k)}) (1 - \tilde{\eta}_v)}{(1 + \theta + \eta^{(k)})} \right\} \quad (E.7) \end{aligned}$$

In the special case of diffusion dominance over recombination, $\theta \gg 1 \gg \eta^{(k)}$, expression (E.7) can be shown to simplify to Eq. (44) in Section (4.a). The total creep strain after N pulses is simply given by adding the individual contributions of each pulse.

$$\varepsilon_{tot}^{(N)} = \sum_{k=1}^N \Delta \varepsilon_p^{(k)} \quad (E.8)$$

NOMENCLATURE

Symbol	Definition	Units
$C_{i,v}$	Point-defect concentration	at/at
$C_{i,v}^{ss}$	Steady-state point-defect concentration	at/at
$D_{i,v}^0$	Point-defect diffusion coefficient pre-exponential	m ² /sec.
$D_{i,v}$	Point-defect diffusion coefficient	m ² /sec.
ρ_d	Dislocation density	m/m ³
ρ_d^A	Density of aligned dislocations	m/m ³
ρ_d^N	Density of non-aligned dislocations	m/m ³
(λ/h)	Ratio of the obstacle spacing to height	m/m
b	Burger vector	m
V_c	Dislocation climb velocity	m/sec.
$Z_{i,v}^0$	Point defect bias in the absence of stress	dimensionless
Z_i^A	Interstitial bias for aligned dislocations	dimensionless
P	Time averaged point defect generation rate	dpa/sec.
α	Recombination coefficient ($\equiv 1/\lambda_{i,v}$)	sec. ⁻¹
$\tau_{i,v}$	Mean diffusion time	sec.
τ_r	Time at which mutual recombination rate = interstitial annihilation rate at sinks	sec.
$\tau_i^{(k)}$	Effective interstitial mean lifetime during the k th pulse in ICFR's	sec.
T_f	Period of the irradiation pulsing	sec.
T_{on}	Pulse on-time	sec.
$T_f - T_{on}$	Pulse off-time	sec.
$\dot{\varepsilon}_p^{(k)}$	Pulsed creep rate during the k th pulse	sec. ⁻¹
$\Delta \varepsilon_p^{(k)}$	The creep increment contributed by the k th pulse	m/m
$\varepsilon_p^{(N)}$	The pulsed creep at the end of N pulses	m/m
k_B	Boltzmann's constant	J/K
T	Temperature	K
$E_{i,v}^m$	Point-defect migration energy	J